



HAL
open science

Robust Flux Reconstruction and a Posteriori Error Analysis for an Elliptic Problem with Discontinuous Coefficients

Daniela Capatina, Aimene Gouasmi, Cuiyu He

► **To cite this version:**

Daniela Capatina, Aimene Gouasmi, Cuiyu He. Robust Flux Reconstruction and a Posteriori Error Analysis for an Elliptic Problem with Discontinuous Coefficients. *Journal of Scientific Computing*, 2023, 98 (1), pp.28. 10.1007/s10915-023-02428-7 . hal-04455830

HAL Id: hal-04455830

<https://hal.science/hal-04455830v1>

Submitted on 4 Mar 2024

HAL is a multi-disciplinary open access archive for the deposit and dissemination of scientific research documents, whether they are published or not. The documents may come from teaching and research institutions in France or abroad, or from public or private research centers.

L'archive ouverte pluridisciplinaire **HAL**, est destinée au dépôt et à la diffusion de documents scientifiques de niveau recherche, publiés ou non, émanant des établissements d'enseignement et de recherche français ou étrangers, des laboratoires publics ou privés.

1 **ROBUST FLUX RECONSTRUCTION AND A POSTERIORI ERROR**
2 **ANALYSIS FOR AN ELLIPTIC PROBLEM WITH DISCONTINUOUS**
3 **COEFFICIENTS**

4 DANIELA CAPATINA *, AIMENE GOUASMI †, AND CUIYU HE‡

5 **Key words.** conforming and nonconforming finite elements, discontinuous coefficients, flux
6 recovery, *a posteriori* error estimation, adaptive mesh refinement

7 **AMS subject classifications.** 65N12, 65N15, 65N30

8 **Abstract.** In this paper, we locally construct a conservative flux for finite element solutions of
9 elliptic interface problems with discontinuous coefficients. Since the Discontinuous Galerkin method
10 has built-in conservative flux, we consider in this paper the conforming Finite Element Method and a
11 special type of nonconforming method with arbitrary orders. We also perform our analysis based on
12 Nitsche's method, which imposes the Dirichlet boundary condition weakly. The construction method
13 is derived based on a mixed problem with one solution coinciding with the finite element solution
14 and with the other solution being naturally used to obtain a conservative flux. We then apply the
15 recovered flux to the *a posteriori* error estimation and prove the robust reliability and efficiency for
16 conforming elements. Numerical experiments are provided to verify the theoretical results.

17 **1. Introduction.** Numerous studies have been conducted to explore the post-
18 processing of conservative fluxes for various purposes, including *a posteriori* error
19 estimation [1, 2], flux conservation in fluid dynamics [3], and super-convergence [4],
20 among others [5, 6, 7, 8, 9, 10]. This paper focuses on designing a locally conservative
21 flux in the $H(\text{div})$ conforming Raviart-Thomas space for finite element solutions of
22 elliptic interface problems, including both conforming and nonconforming approxima-
23 tions with arbitrary polynomial degree $k \in \mathbb{N}^*$. The recovered flux is then applied
24 and analyzed in a *a posteriori* error estimation, which plays a crucial role in adaptive
25 methods.

26 Equilibrated *a posteriori* error estimators have attracted much interest due to the
27 guaranteed reliability bound with the reliability constant equal to one. This property
28 implies that they are perfect for discretization error control on both coarse and fine
29 meshes. It is important to note that error control on coarse meshes is important but
30 difficult for computationally challenging problems.

31 For the conforming finite element approximation, a mathematical foundation of
32 equilibrated estimators is the Prager-Syngé identity [11]. Based on this identity,
33 various equilibrated estimators have been studied by many researchers (see, e.g., [1,
34 12, 13, 14, 2, 15, 16, 17, 18, 6, 19, 8, 10, 3, 20, 9]). The key ingredient for continuous
35 finite elements is a recovered equilibrated (locally conservative) flux in the $H(\text{div}; \Omega)$
36 space based on the numerical flux which is typically neither in the $H(\text{div}; \Omega)$ space nor
37 locally conservative. Using a partition of unity, Ladevèze and Leguillon [1] initiated
38 a local procedure to reduce the construction of an equilibrated flux to vertex patch-
39 based local calculations. For the continuous linear finite element approximation to the
40 Poisson equation in two dimensions, an equilibrated flux in the lowest order Raviart-
41 Thomas space was explicitly constructed in [18]. This explicit approach does not

*LMAP & CNRS UMR 5142, University of Pau and Pays de l'Adour, IPRA BP 1155, 64013 Pau,
France (daniela.capatina@univ-pau.fr)

†LMAP & CNRS UMR 5142, University of Pau and Pays de l'Adour, IPRA BP 1155, 64013 Pau,
France (aimene.gouasmi@univ-pau.fr)

‡Department of Mathematics, Oklahoma State University, Stillwater, OK, USA, 74078
(cuiyu.he@okstate.edu)

42 lead to a robust equilibrated estimator with respect to the coefficient jump without
 43 introducing a constraint minimization (see [8]). The constraint minimization on each
 44 vertex-based patch may be solved by first computing an equilibrated flux and then
 45 calculating a divergence-free correction, see [20] and references therein. In [9], a
 46 unified method also based on the partition of unity was developed. This method
 47 requires solving local mixed problems on a vertex patch for each vertex. In [16, 3] a
 48 global problem is solved on the enriched piecewise constant DG space to obtain the
 49 conservative flux, which is relatively more computationally expensive.

50 Partition of unity is a commonly used tool for localization. In principle, it can be
 51 uniformly applied to various finite element methods. However, it is studied mainly
 52 for the continuous Galerkin method since explicit recovery for its solution has been a
 53 challenging research topic due to the continuity of the finite element space. Existing
 54 methods using partition of unity are relatively complex since it requires solving star-
 55 patched local problems that are either constrained [8] or in a mixed form [9].

56 For an exception apart from the partition of unity, we refer to [10] where two-
 57 dimensional Poisson problems are studied. This method is based on a unified mixed
 58 problem equivalent to conforming, nonconforming and discontinuous Galerkin meth-
 59 ods. The idea is to use the Lagrange multiplier, defined on the facets of the mesh, as
 60 a correction of the degrees of freedom of the flux. The choice of the multiplier's space
 61 is fundamental since it should satisfy the uniform inf-sup condition and enable local
 62 construction. With this approach, one only needs to solve an explicit low-dimensional
 63 linear system for each vertex. It has recently been extended to unfitted methods [21].

64 In this study, we adopt a similar approach for the diffusion problem where the
 65 diffusion coefficients may undergo large jumps along the interfaces. As a result, the
 66 auxiliary mixed formulation and the local construction of its Lagrange multiplier
 67 resemble those in [10]. Our main contribution is to achieve robustness concerning the
 68 discontinuous coefficients by properly designing the algorithm and analysis.

69 Firstly, we consider the conforming finite element method, which is the most diffi-
 70 cult case for the flux reconstruction. We use triangular meshes and Nitsche's method
 71 to treat the Dirichlet boundary conditions; note that in [10], the Dirichlet condition
 72 was treated strongly. We provide a well-posed equivalent mixed formulation, where
 73 the continuity of the solution and of the test-functions across the interior sides of the
 74 mesh is imposed weakly. We obtained the robust inf-sup constant in terms of the coef-
 75 ficients, and we establish a local bound for the multiplier (and hence, for the recovered
 76 flux) with a constant whose dependence on the coefficients is given explicitly. This
 77 type of result is new, at the best of our knowledge; for quasi-monotone coefficients,
 78 we retrieve the robustness already known in the literature for other reconstructions
 79 in this case.

80 Secondly, we consider a nonconforming finite element approximation of arbitrary
 81 polynomial degree $k \in \mathbb{N}^*$, based on the space introduced by Matthies and Tobiska
 82 [22]. The standard nonconforming space of odd degree rises with no particular dif-
 83 ficulty, and the reconstruction of conservative fluxes, in this case, is well-known in
 84 the literature. Meanwhile, this is no longer true for an even degree k , due to the
 85 loss of insolvency cf. [23]. The main advantages of the finite elements proposed in
 86 [22] are that they are uniformly defined for any k and are also inf-sup stable for the
 87 Stokes problem. Our contribution consists in extending the approach of [10] to these
 88 spaces in a completely robust way with respect to the diffusion coefficients. To our
 89 knowledge, flux reconstruction for this type of nonconforming finite element is new.

90 An important use of flux recovery is in the estimation of a posteriori errors, where

91 the weighted L_2 -norm of the difference between the numerical flux and the recovered
 92 flux can be employed. This technique is particularly valuable in adaptive mesh refine-
 93 ment procedures, commonly employed for problems with singularities, discontinuities,
 94 or sharp derivatives. The study of a posteriori error estimation has been an active
 95 area of research for several decades, as demonstrated by the extensive literature on
 96 the topic (see, for example, [2, 24, 7]).

97 In this paper, we carry out the a posteriori error analysis for the conforming case,
 98 tracking the dependence of the constants involved in the error bounds on the diffusion
 99 coefficients. We establish the sharp reliability of the a posteriori error indicator and its
 100 robust local efficiency in the case of quasi-monotone coefficients. Finally, we present
 101 several numerical experiments illustrating the theoretical results for a piecewise linear
 102 continuous method.

103 The paper is organized as follows. In Section 2, we give the model problem and
 104 its weak formulation. We present in Section 3 the conforming and nonconforming
 105 finite element approximations and their equivalent mixed formulations, for which we
 106 establish the well-posedness. For both discretizations, the local computation and
 107 robust bound of the multipliers are detailed in Section 4, whereas the definition of the
 108 conservative fluxes is given in Section 5. Section 6 deals with the a posteriori error
 109 estimation for the conforming approximation by means of the recovered flux. Finally,
 110 Section 7 is devoted to the numerical tests, while in the Appendix we give the proof
 111 of the inf-sup condition for the conforming method.

112 **Data Availability.** No data is available. Enquiries about the code should be
 113 directed to the authors.

114 **Ethics declaration.** The authors declare that they have no conflict of interest.

115 **2. Model problem and notation.** Let Ω be a bounded domain of \mathbb{R}^2 with
 116 polygonal boundary $\partial\Omega$ with exterior unit normal n . Let $\partial\Omega = \Gamma_D \cup \Gamma_N$, where
 117 Γ_D and Γ_N are disjoint and, for the sake of simplicity, $|\Gamma_D| > 0$. We consider the
 118 following model problem: find $u : \Omega \rightarrow \mathbb{R}$ such that

$$\begin{aligned} -\operatorname{div}(K\nabla u) &= f && \text{in } \Omega \\ u &= g_D && \text{on } \Gamma_D \\ K\nabla u \cdot n &= g_N && \text{on } \Gamma_N. \end{aligned} \quad (2.1)$$

Assume that $f \in L^2(\Omega)$, $g_N \in L^2(\Gamma_N)$, $g_D \in H^{1/2}(\Gamma_D)$ and that K is a symmetric positive definite 2×2 matrix, of coefficients in $L^\infty(\Omega)$. For the sake of simplicity, we take in what follows $K = k\mathbb{I}_2$ with $k \in L^\infty(\Omega)$ and $k(x) \geq k_0 > 0$ a.e in Ω . For any $\chi \in H^{1/2}(\Gamma_D)$, let

$$V^\chi = \{v \in H^1(\Omega) : v = \chi \text{ on } \Gamma_D\}.$$

The primal weak formulation associated to the previous boundary problem reads:

$$u \in V^{g_D}, \quad a(u, v) = (f, v)_\Omega + (g_N, v)_{\Gamma_N} \quad \forall v \in V^0,$$

119 where $a(u, v) = (K\nabla u, \nabla v)_\Omega$. Thanks to the Lax-Milgram lemma, there exists a
 120 unique solution to this problem.

121 In the following, we introduce some notation. We denote by \mathcal{T}_h a regular mesh
 122 consisting of triangles, such that the domain's boundary $\partial\Omega$ is covered by the Dirichlet
 123 and Neumann sides, \mathcal{F}_h^D and \mathcal{F}_h^N , respectively. We denote by \mathcal{F}_h^{int} the set of interior
 124 sides and we put $\mathcal{F}_h = \mathcal{F}_h^{int} \cup \mathcal{F}_h^D$. We denote by \mathcal{N}_h^{int} and \mathcal{N}_h^∂ the set of nodes which

125 are interior to the domain Ω or situated on $\partial\Omega$, respectively. We assume, for the sake
126 of simplicity, that a cell $T \in \mathcal{T}_h$ cannot have all three vertices on Γ_N .

127 For a interior side F , n_F is a fixed, arbitrary, unit vector normal to F , oriented
128 from T^- towards T^+ , where T^-, T^+ are the two triangles sharing the side F . If the
129 side F lies on $\partial\Omega$, we set $n_F = n$.

We define the following spaces of piecewise polynomial functions of degree $l \in \mathbb{N}$
on the cells and the sides, respectively :

$$\begin{aligned} \mathcal{D}_h^l &= \{v_h \in L^2(\mathcal{T}_h) : v_h|_T \in P^l(T) \quad \forall T \in \mathcal{T}_h\}, \\ \mathcal{C}_h^l &= \mathcal{D}_h^l \cap C^0(\bar{\Omega}), \\ \mathcal{M}_h^l &= \{\mu_h \in L^2(\mathcal{F}_h^{int}) : \mu_h|_F \in P^l(F) \quad \forall F \in \mathcal{F}_h^{int}\}. \end{aligned}$$

For the sake of simplicity, we assume that K is piecewise constant. Let $v \in \mathcal{D}_h^l$.
For a given $F \in \mathcal{F}_h^{int}$ and $x \in F$, we define as usually:

$$v_F^+(x) = \lim_{\varepsilon \rightarrow 0^+} v(x + \varepsilon n_F), \quad v_F^-(x) = \lim_{\varepsilon \rightarrow 0^+} v(x - \varepsilon n_F),$$

as well as the jump and weighted means at $x \in F$, by

$$[v]_F = v_F^- - v_F^+, \quad \{v\}_F = \omega^+ v_F^+ + \omega^- v_F^-, \quad \{v\}_F^* = \omega^- v_F^+ + \omega^+ v_F^-,$$

130 where (cf. for instance [25]):

$$\omega^+ = \frac{k^-}{k^+ + k^-}, \quad \omega^- = \frac{k^+}{k^+ + k^-}, \quad k^\pm = k|_{T^\pm}. \quad (2.2)$$

131 We also introduce the stabilisation parameter $k_F = \frac{k^+ k^-}{k^+ + k^-}$. For a boundary side
132 F , we set $[v]_F = \{v\}_F = v_F^-$ and $k_F = k^-$. It is useful to note that, for any $F \in \mathcal{F}_h$,

$$0 \leq \omega^\pm \leq 1, \quad \omega^+ + \omega^- = 1, \quad k_F = k^\pm \omega^\pm \leq k^\pm. \quad (2.3)$$

In the sequel, we will omit the index F in the jump and the means whenever
possible. We will also use the following notation for the piecewise integration:

$$\int_{\mathcal{T}_h} = \sum_{T \in \mathcal{T}_h} \int_T, \quad \int_{\mathcal{F}_h} = \sum_{F \in \mathcal{F}_h} \int_F.$$

133 We recall the well-known trace inequality, for $T \in \mathcal{T}_h$ and $F \subset \partial T$:

$$|F|^{-1/2} \|v\|_{0,F} \lesssim \frac{1}{d_T} \|v\|_{0,T} + |v|_{1,T}, \quad \forall v \in H^1(T). \quad (2.4)$$

134 **3. Discrete problem and equivalent mixed formulation.** We consider suc-
135 cessively conforming and nonconforming finite element discretizations.

3.1. Conforming approximation. We first discretize problem (2.1) by means
of conforming finite elements. We use Nitsche's method to treat the Dirichlet bound-
ary condition. For the simplicity of presentation, we consider in what follows the
piecewise linear case ($l = 1$) but the theory holds for arbitrary $l \in \mathbb{N}^*$, cf. [10] for the

Poisson equation. Let the bilinear and linear forms, for any $u_h, v_h \in \mathcal{C}_h^1$:

$$\begin{aligned} a_h(u_h, v_h) &= \int_{\mathcal{T}_h} K \nabla u_h \cdot \nabla v_h \, dx - \int_{\mathcal{F}_h^D} (K \nabla u_h \cdot n v_h + K \nabla v_h \cdot n u_h) \, ds \\ &\quad + \gamma \int_{\mathcal{F}_h^D} \frac{k_F}{|F|} v_h u_h \, ds, \\ l_h(v_h) &= \int_{\mathcal{T}_h} f v_h \, dx + \int_{\Gamma_N} g_N v_h \, ds - \int_{\mathcal{F}_h^D} K \nabla v_h \cdot n g_D \, ds + \gamma \int_{\mathcal{F}_h^D} \frac{k_F}{|F|} v_h g_D \, ds, \end{aligned}$$

136 where $\gamma > 0$ is a stabilisation parameter independent of h and K .

137 We consider the discrete problem:

$$u_h \in \mathcal{C}_h^1, \quad a_h(u_h, v_h) = l_h(v_h) \quad \forall v_h \in \mathcal{C}_h^1. \quad (3.1)$$

We use the following semi-norm and norm on $H^1(\Omega)$:

$$|v|_{1,K} = \|K^{1/2} \nabla v\|_{0,\Omega}, \quad \|v\| = \left(|v|_{1,K}^2 + \int_{\mathcal{F}_h^D} \frac{k_F}{|F|} v^2 \, ds \right)^{1/2}.$$

138 It is well-known that for γ large enough, $a_h(\cdot, \cdot)$ is $\|\cdot\|$ -coercive on $\mathcal{C}_h^1 \times \mathcal{C}_h^1$, uniformly
139 with respect to both h and K . The existence and uniqueness of the solution of (3.1)
140 follows from the Lax-Milgram lemma.

141 Following [10], we introduce a hybrid mixed formulation with an additional un-
142 known θ_h defined on the interior sides of the mesh. The continuity of u_h across the
143 interior sides is dualized by means of a multiplier. Note that in [10], the Dirichlet
144 boundary condition was imposed strongly, leading to a multiplier defined on both the
145 interior and the Dirichlet sides.

The multiplier θ_h is then used in order to recover the numerical conservative flux.
It is important to note that we do not solve the global mixed formulation, but we
compute θ_h locally. For this purpose, let us first introduce the space

$$\mathcal{M}_h = \left\{ \mu_h \in \mathcal{M}_h^1; \sum_{F \in \mathcal{F}_N} \mathfrak{s}_{N,F} |F| \mu_h|_F(N) = 0 \quad \forall N \in \mathcal{N}_h^{int} \right\},$$

146 where \mathcal{F}_N is the set of sides sharing the node $N \in \mathcal{N}_h^{int}$ and $\mathfrak{s}_{N,F}$ is the sign function,
147 which is equal to 1 or -1 depending upon the orientation of n_F with respect to the
148 clockwise rotation sense around N . The auxiliary mixed formulation is given by: find
149 $(\tilde{u}_h, \theta_h) \in \mathcal{D}_h^1 \times \mathcal{M}_h$ such that

$$\begin{aligned} \tilde{a}_h(\tilde{u}_h, v_h) + b_h(\theta_h, v_h) &= l_h(v_h) \quad \forall v_h \in \mathcal{D}_h^1, \\ b_h(\mu_h, \tilde{u}_h) &= 0 \quad \forall \mu_h \in \mathcal{M}_h, \end{aligned} \quad (3.2)$$

where

$$\begin{aligned} \tilde{a}_h(\tilde{u}_h, v_h) &= a_h(\tilde{u}_h, v_h) - \int_{\mathcal{F}_h^{int}} \{K \nabla \tilde{u}_h \cdot n_F\} [v_h] \, ds - \int_{\mathcal{F}_h^{int}} \{K \nabla v_h \cdot n_F\} [\tilde{u}_h] \, ds, \\ b_h(\mu_h, v_h) &= \sum_{F \in \mathcal{F}_h^{int}} \frac{k_F |F|}{2} \sum_{N \in \mathcal{N}_F} \mu_h|_F(N) [v_h]_F(N), \end{aligned}$$

with \mathcal{N}_F the set of vertices of F . Note that $b_h(\mu_h, v_h)$ is the approximation of
 $\int_{\mathcal{F}_h^{int}} k_F \mu_h [v_h] ds$ by the trapeze formula (or, for an arbitrary degree l , by the Gauss-
 Lobatto integration formula with $l + 1$ points).

We first show that the solution \tilde{u}_h of the mixed formulation (3.2) coincides with
 the solution u_h of the original discrete problem (3.1).

LEMMA 3.1. *The discrete kernel of $b_h(\cdot)$ coincides with the space \mathcal{C}_h^1 , i.e.,*

$$\text{Ker } b_h = \{v_h \in \mathcal{D}_h^1; b_h(\mu_h, v_h) = 0, \quad \forall \mu_h \in \mathcal{M}_h\} = \mathcal{C}_h^1.$$

Proof. Obviously, $\mathcal{C}_h^1 \subset \text{Ker } b_h$. Now let any $v_h \in \text{Ker } b_h$ and consider the function
 μ_h defined by $\mu_h|_F = |F|^{-1}[v_h]|_F$ for any $F \in \mathcal{F}_h^{int}$. Clearly, μ_h belongs to \mathcal{M}_h because

$$\forall N \in \mathcal{N}_h^{int}, \quad \sum_{F \in \mathcal{F}_N} \mathfrak{s}_{N,F} |F| \mu_h|_F(N) = \sum_{F \in \mathcal{F}_N} \mathfrak{s}_{N,F} [v_h]|_F = 0.$$

From $b_h(\mu_h, v_h) = 0$ we get $[v_h]|_F = 0$ for any $F \in \mathcal{F}_h^{int}$, which yields $v_h \in \mathcal{C}_h^1$. \square

Thus, \tilde{u}_h satisfies (3.1) and the uniqueness of its solution yields $\tilde{u}_h = u_h$.

We next establish the well-posedness of the mixed formulation. For this purpose,
 we introduce the following discrete norms:

$$\|v_h\|_h = \left(\int_{\mathcal{T}_h} K \nabla v_h \cdot \nabla v_h dx + \int_{\mathcal{F}_h} |F|^{-1} k_F [v_h]^2 ds \right)^{1/2}, \quad v_h \in \mathcal{D}_h^1,$$

$$\|\mu_h\|_{\mathcal{M}_h} = \left(\int_{\mathcal{F}_h^{int}} |F| k_F \mu_h^2 ds \right)^{1/2}, \quad \mu_h \in \mathcal{M}_h^1$$

and we recall the following inequality (see for instance [7]), which holds uniformly
 with respect to h and K :

$$\forall v_h \in \mathcal{D}_h^1, \quad \int_{\mathcal{F}_h} |F| k_F^{-1} \{K \nabla v_h \cdot n_F\}^2 ds \lesssim \int_{\mathcal{T}_h} K \nabla v_h \cdot \nabla v_h dx. \quad (3.3)$$

Thanks to (3.3) and to the Cauchy-Schwarz inequality, one immediately obtains the
 uniform continuity of the bilinear forms: for any $\mu_h \in \mathcal{M}_h$ and $u_h, v_h \in \mathcal{D}_h^1$,

$$\tilde{a}_h(u_h, v_h) \lesssim \|u_h\|_h \|v_h\|_h, \quad b_h(\mu_h, v_h) \lesssim \|v_h\|_h \|\mu_h\|_{\mathcal{M}_h}.$$

Lemma 3.1 yields the uniform $\|\cdot\|_h$ -coercivity of $\tilde{a}_h(\cdot, \cdot)$ on $\text{Ker } b_h$ for γ large enough.
 In order to apply the Babuska-Brezzi theorem to the mixed problem (3.2), we establish
 the inf-sup condition for $b_h(\cdot, \cdot)$. The proof is similar to [10] for the Poisson problem
 and is given in the Appendix. The difference is that we track the robust dependence
 of the inf-sup constant on the diffusion coefficient K .

DEFINITION 3.2. *K is quasi-monotone on ω_N if there exists a clockwise or
 counter-clockwise complete path along which K is monotone. K is said to be quasi-
 monotone on \mathcal{T}_h if it is quasi-monotone for every $\omega_N, N \in \mathcal{N}_h$.*

LEMMA 3.3. *Assume K is quasi-monotone. There exists a constant $\beta > 0$
 independent of h, γ and K such that*

$$\inf_{\mu_h \in \mathcal{M}_h} \sup_{v_h \in \mathcal{D}_h^1} \frac{b_h(\mu_h, v_h)}{\|\mu_h\|_{\mathcal{M}_h} \|v_h\|_h} \geq \beta.$$

The proof of the lemma is provided in the appendix.

168 **3.2. Nonconforming approximation.** We now consider a nonconforming ap-
 169 proximation based on the finite element space of arbitrary polynomial degree $k \in \mathbb{N}^*$
 170 introduced in [22]. We begin by recalling its definition. Let $T \in \mathcal{T}_h$ and let

$$\Sigma_{k+1}(T) = \text{span}\{b_T \varphi_{T,1}^{k-2-i} \varphi_{T,2}^i; i = 0, \dots, k-2\} \subset P^{k+1}(T), \quad (3.4)$$

where $\{\varphi_{T,i}; 1 \leq i \leq 3\}$ denote the barycentric coordinates of the triangle T and

$$b_T = (\varphi_{T,1} - \varphi_{T,2})(\varphi_{T,2} - \varphi_{T,3})(\varphi_{T,3} - \varphi_{T,1}).$$

Consider the following enriched space

$$V_k(T) = P^k(T) \oplus \Sigma_{k+1}(T)$$

171 and define the nodal basis functions as follows:

$$\begin{aligned} N_{F,i}^T(v) &= \frac{1}{|F|} \int_F v L_i ds, \quad 0 \leq i \leq k-1, \quad F \in \mathcal{F}_h \cap \partial T \\ N_j^T(v) &= \frac{1}{|T|} \int_T v M_j^T dx, \quad 1 \leq j \leq \frac{k(k-1)}{2}, \end{aligned} \quad (3.5)$$

172 where $\{M_j^T\}$ is an arbitrary but fixed basis of $P^{k-2}(T)$ and L_j is the j -th order
 173 Legendre polynomial. Let $\phi_{F,i}$, for $0 \leq i \leq k-1$ and ϕ_j , for $1 \leq j \leq \frac{k(k-1)}{2}$ be the
 174 corresponding nodal basis functions.

The discontinuous and nonconforming spaces \mathcal{DG}_h^k and \mathcal{NC}_h^k are defined as follows:

$$\begin{aligned} \mathcal{DG}_h^k &= \{v_h \in L^2(\Omega); v_h|_T \in V_k(T), \forall T \in \mathcal{T}_h\}, \\ \mathcal{NC}_h^k &= \left\{ v_h \in \mathcal{DG}_h^k; \int_F [v_h] p ds = 0, \forall F \in \mathcal{F}_h^{int}, \forall p \in P^{k-1}(F) \right\}. \end{aligned}$$

175 We consider the following discrete version of (2.1): find $u_h^* \in \mathcal{NC}_h^k$ such that

$$a_h(u_h^*, v_h) = l_h(v_h) \quad \forall v_h \in \mathcal{NC}_h^k, \quad (3.6)$$

176 which is well-posed. We introduce the auxiliary mixed formulation: find $(\tilde{u}_h^*, \theta_h^*) \in$
 177 $\mathcal{DG}_h^k \times \mathcal{M}_h^{k-1}$ such that

$$\begin{aligned} \tilde{a}_h^*(\tilde{u}_h^*, v_h) + b_h^*(\theta_h^*, v_h) &= l_h(v_h) \quad \forall v_h \in \mathcal{DG}_h^k, \\ b_h^*(\mu_h, \tilde{u}_h^*) &= 0 \quad \forall \mu_h \in \mathcal{M}_h^{k-1}, \end{aligned} \quad (3.7)$$

where

$$\begin{aligned} \tilde{a}_h^*(\tilde{u}_h^*, v_h) &= a_h(\tilde{u}_h^*, v_h) - \int_{\mathcal{F}_h^{int}} \left(\pi_F^{k-1} \{K \nabla \tilde{u}_h^* \cdot n_F\} [v_h] + \pi_F^{k-1} \{K \nabla v_h \cdot n_F\} [\tilde{u}_h^*] \right) ds, \\ b_h^*(\mu_h, v_h) &= \int_{\mathcal{F}_h^{int}} \mu_h [v_h] ds \end{aligned}$$

178 and where π_F^{k-1} stands for the $L^2(F)$ -orthogonal projection on $P^{k-1}(F)$.

Note that one is now able to get rid of the coefficient k_F in the bilinear form $b_h^*(\cdot, \cdot)$ because there is no linear constraint in the space \mathcal{M}_h^{k-1} . Since the multipliers are P^{k-1} -functions on each interior side, we immediately obtain that

$$\text{Ker } b_h^* = \left\{ v_h \in \mathcal{DG}_h^k : b_h^*(\mu_h, v_h) = 0, \quad \forall \mu_h \in \mathcal{M}_h^{k-1} \right\} = \mathcal{NC}_h^k.$$

179 So the primal and mixed formulations (3.6) and (3.7) are equivalent, i.e. $\tilde{u}_h^* = u_h^*$.

We are next interested in the well-posedness of the mixed formulation (3.7). The continuity of $\tilde{a}_h^*(\cdot, \cdot)$ is similar to the conforming case. The space \mathcal{M}_h^{k-1} is now endowed with the norm:

$$\|\mu_h\|_{\mathcal{N}\mathcal{C}_h}^2 = \int_{\mathcal{F}_h^{int}} k_F^{-1} |F| \mu_h^2 ds, \quad \forall \mu_h \in \mathcal{M}_h^{k-1},$$

180 which immediately yields $b_h^*(\mu_h, v_h) \leq \|\mu_h\|_{\mathcal{N}\mathcal{C}_h} \|v_h\|_h$. So we only have to establish
181 the inf-sup condition for $b_h^*(\cdot, \cdot)$.

LEMMA 3.4. *There exists a constant β^* independent of h , γ and K such that*

$$\inf_{\mu_h \in \mathcal{M}_h^{k-1}} \sup_{v_h \in \mathcal{D}\mathcal{G}_h^k} \frac{b_h^*(\mu_h, v_h)}{\|\mu_h\|_{\mathcal{N}\mathcal{C}_h} \|v_h\|_h} \geq \beta^*.$$

182 *Proof.* We construct a Fortin operator, which associates to any $\mu_h \in \mathcal{M}_h^{k-1}$ a
183 unique function $v_h \in \mathcal{D}\mathcal{G}_h^k$ satisfying

$$b_h^*(\mu_h, v_h) \gtrsim \|\mu_h\|_{\mathcal{N}\mathcal{C}_h}^2, \quad \|v_h\|_h \lesssim \|\mu_h\|_{\mathcal{N}\mathcal{C}_h}. \quad (3.8)$$

184 For any $F \in \mathcal{F}_h^{int}$, let $\Delta_F = T^+ \cup T^-$ the patch consisting of the triangles sharing
185 the side F . The construction of v_h is achieved patch-wise: $v_h = \sum_{F \in \mathcal{F}_h^{int}} v_F$ with v_F

186 defined on Δ_F . Since $\mu_h|_F \in P^{k-1}$, we can write it in the Legendre basis of P^{k-1} :

$$\exists! (\alpha_0, \dots, \alpha_{k-1}) \in \mathbb{R}^k, \quad \mu_h|_F = \sum_{j=0}^{k-1} \alpha_j L_j.$$

187 Then we define v_F as follows:

$$(v_F)|_{T^+} = \frac{|F|}{k^+} \sum_{i=0}^{k-1} \alpha_i \phi_{F,i}, \quad (v_F)|_{T^-} = \frac{|F|}{k^-} \sum_{i=0}^{k-1} \alpha_i \phi_{F,i}. \quad (3.9)$$

This choice directly yields that $v_F \in \mathcal{D}\mathcal{G}_h^k$ and $[v_h]|_F = k_F^{-1} |F| \sum_{i=0}^{k-1} \alpha_i \phi_{F,i}$. Hence,

$$\int_F \mu_h [v_h] ds = k_F^{-1} |F| \sum_{i,j=0}^{k-1} \alpha_i \alpha_j \int_F L_j \phi_{F,i} ds = k_F^{-1} |F|^2 \sum_{j=0}^{k-1} \alpha_j^2,$$

188 thanks to the definition of the nodal basis functions $\phi_{F,i}$. Noting that

$$\int_F \mu_h^2 ds = \int_F \left(\sum_{j=0}^{k-1} \alpha_j L_j \right)^2 ds = \sum_{j=0}^{k-1} \alpha_j^2 \|L_j\|_{0,F}^2 \approx |F| \sum_{j=0}^{k-1} \alpha_j^2, \quad (3.10)$$

189 we deduce that

$$b_h^*(\mu_h, v_h) = \sum_{F \in \mathcal{F}_h^{int}} \int_F \mu_h [v_h] ds \approx \|\mu_h\|_{\mathcal{N}\mathcal{C}_h}^2. \quad (3.11)$$

We still have to establish the second bound of (3.8). For any $F \in \mathcal{F}_h^{int}$, we have that:

$$\frac{k_F}{|F|} \|[v_h]\|_{0,F}^2 \leq \frac{|F|}{k_F} \left(\sum_{i=0}^{k-1} \alpha_i^2 \right) \left(\sum_{i=0}^{k-1} \|\phi_{F,i}\|_{0,F}^2 \right) \lesssim \frac{|F|^2}{k_F} \sum_{i=0}^{k-1} \alpha_i^2 \lesssim \frac{|F|}{k_F} \|\mu_h\|_{0,F}^2.$$

190 A similar bound is obtained on any Dirichlet side, which finally leads to

$$\int_{\mathcal{F}_h} k_F |F|^{-1} [v_h]^2 \lesssim \|\mu_h\|_{\mathcal{NC}_h}^2. \quad (3.12)$$

We next have, using first $(v_h)|_T = \sum_{F \in \partial T \cap \mathcal{F}_h^{int}} v_F$ and then (3.9), that

$$\begin{aligned} \int_{\mathcal{T}_h} K \nabla v_h \cdot \nabla v_h dx &= \sum_{T \in \mathcal{T}_h} k_T |v_h|_{1,T}^2 \lesssim \sum_{F \in \mathcal{F}_h^{int}} \sum_{T \in \Delta_F} k_T |v_F|_{1,T}^2 \\ &\leq \sum_{F \in \mathcal{F}_h^{int}} \sum_{T \in \Delta_F} \frac{|F|^2}{k_T} \left(\sum_{i=0}^{k-1} |\alpha_i| |\phi_{F,i}|_{1,T} \right)^2. \end{aligned}$$

191 Since $|\phi_{F,i}|_{1,T} \leq C$ and $k_F \leq k^\pm$, it follows thanks to (3.10) that

$$\int_{\mathcal{T}_h} K \nabla v_h \cdot \nabla v_h dx \lesssim \sum_{F \in \mathcal{F}_h^{int}} \frac{|F|^2}{k_F} \left(\sum_{i=0}^{k-1} \alpha_i^2 \right) \lesssim \sum_{F \in \mathcal{F}_h^{int}} \frac{|F|}{k_F} \|\mu_h\|_{0,F}^2 = \|\mu_h\|_{\mathcal{NC}_h}^2. \quad (3.13)$$

192 We can now conclude thanks to (3.11), (3.12) and (3.13). \square

193 **4. Local computation of the multiplier.** Again, we discuss successively the
194 conforming and nonconforming cases.

4.1. Conforming approximation. Let the functional

$$r_h(\cdot) = l_h(\cdot) - \tilde{a}_h(u_h, \cdot).$$

195 Thanks to the mixed formulation, we have $r_h(v_h) = 0$ for any $v_h \in \mathcal{C}_h^1$. Moreover, θ_h
196 is uniquely defined in \mathcal{M}_h by

$$b_h(\theta_h, v_h) = r_h(v_h) \quad \forall v_h \in \mathcal{D}_h^1. \quad (4.1)$$

It is useful to introduce, for any interior side F of vertices N, M , the bilinear form

$$b_F(\theta, \varphi) = \frac{|F|k_F}{2} (\theta(N)\varphi(N) + \theta(M)\varphi(M)).$$

197 Let $N \in \mathcal{N}_h$. We define $\theta_N \in \mathcal{M}_h$ on $\mathcal{F}_N \cap \mathcal{F}_h^{int}$ such that, for any $T \in \omega_N$,

$$b_h(\theta_N, \varphi_N \chi_T) = r_h(\varphi_N \chi_T), \quad (4.2)$$

$$b_h(\theta_N, \varphi_M \chi_T) = 0, \quad \forall M \in \mathcal{N}_T \setminus \{N\} \quad (4.3)$$

198 with φ_N, φ_M the P^1 -nodal basis functions and χ_T the characteristic function on T .
199 We impose moreover $\theta_N = 0$ on $\mathcal{F}_h^{int} \setminus \mathcal{F}_N$.

200 The next result shows that the multiplier θ_h can be computed locally. We refer
201 to [10] for the proof, which is based on (4.1).

202 LEMMA 4.1. Let θ_h and θ_N be the solutions of (3.2) and (4.2)-(4.3), respectively.
 203 Then

$$\theta_h = \sum_{N \in \mathcal{N}_h} \theta_N. \quad (4.4)$$

204 In what follows, we study the linear system (4.2)-(4.3). Note that (4.3) immedi-
 205 ately yields $(\theta_N)|_F(M) = 0$ for all $F \in \mathcal{F}_N$, where M denotes the other vertex of F ;
 206 thus, θ_N obviously satisfies the constraint of the space \mathcal{M}_h at all the interior nodes
 207 M different from N . Therefore, we only need to consider (4.2). As in [10], it can be
 208 shown that it has a unique solution in \mathcal{M}_h .

209 We next focus on the bound of θ_N . For this purpose, let n_N denote the number
 210 of elements in ω_N , ordered clockwise from T_1 to T_{n_N} , with T_1 the element such that
 211 $k|_{T_1} = \max_{T \in \omega_N} k_T$ if N is a interior node and T_1 containing a boundary side otherwise.
 212 We set $F_i = \partial T_i \cap \partial T_{i+1}$, with $T_{n_N+1} = T_1$ and $i \in \{1, \dots, n_N\}$ if $N \in \mathcal{N}_h^{int}$, and
 213 $i \in \{1, \dots, n_N-1\}$ if $N \in \mathcal{N}_h^\partial$. We recall that the sign coefficient $\mathfrak{s}_i := \mathfrak{s}_{N, F_i}$ equals ± 1 if
 214 $T_i = T^\mp$ with respect to F_i . Let also $x_i := \mathfrak{s}_i k_{F_i} |F_i| (\theta_N)|_{F_i}(N)$ and $b_i := 2r_h(\varphi_N \chi_{T_i})$.

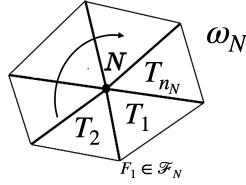


Fig. 4.1: Patch ω_N around a node N

215 We now introduce the following constant, for any $N \in \mathcal{N}_h$:

$$C_N := \max_{1 \leq j \leq i \leq n_N} \frac{\sqrt{k_i}}{\sqrt{k_j}} \quad \text{where} \quad k_i = k|_{T_i}. \quad (4.5)$$

216 Clearly, $C_N = 1$ if the coefficient K is quasi-monotone.

217 For $N \in \mathcal{N}_h^{int}$, the local system (4.2) together with the condition $\theta_N \in \mathcal{M}_h$
 218 translates into the following matrix equation:

$$x_i - x_{i-1} = 2b_i \quad (1 \leq i \leq n_N), \quad \sum_{i=1}^{n_N} k_{F_i}^{-1} x_i = 0, \quad (4.6)$$

219 where $x_0 = x_{n_N}$. A simple calculation yields that the solution of (4.6) is given by:

$$x_i = \sum_{j=1}^i \frac{\bar{\Lambda}_j}{\Lambda_1} b_j - \sum_{j=i+1}^{n_N} \frac{\Lambda_j}{\Lambda_1} b_j, \quad 1 \leq i < n_N, \quad x_{n_N} = \sum_{j=1}^{n_N} \frac{\bar{\Lambda}_j}{\Lambda_1} b_j, \quad (4.7)$$

220 where $\Lambda_j = \sum_{l=j}^{n_N} k_{F_l}^{-1}$, $\bar{\Lambda}_j = \Lambda_1 - \Lambda_j$ for $1 \leq j \leq n_N$.

221 For $N \in \mathcal{N}_h^\partial$, since θ_N is defined only on the interior sides and no constraint at
 222 the node N is imposed in the space \mathcal{M}_h , system (4.2) translates into:

$$x_i - x_{i-1} = 2b_i \quad (1 \leq i \leq n_N - 1) \quad (4.8)$$

223 where $x_0 = 0$ here. Its solution is given by $x_i = 2 \sum_{j=1}^i b_j = -2 \sum_{j=i+1}^{n_N} b_j$ for $1 \leq i \leq n_N - 1$.

224 LEMMA 4.2. For any $N \in \mathcal{N}_h$, we have that:

$$k_{F_i}^{-1/2} |x_i| \lesssim \mathcal{C}_N \sum_{j=1}^{n_N} k_j^{-1/2} |b_j|, \quad 1 \leq i \leq n_N. \quad (4.9)$$

Proof. We detail the proof for $N \in \mathcal{N}_h^{int}$, the case of a boundary node being similar. By using that $0 < \frac{\Lambda_j}{\Lambda_1} \leq 1$ for $2 \leq j \leq n_N$, we first get from (4.7) that $|x_1| \leq \sum_{j=2}^{n_N} |b_j|$, which gives that

$$k_{F_1}^{-1/2} |x_1| \leq \sum_{j=2}^{n_N} (k_{F_1}^{-1/2} k_j^{1/2}) k_j^{-1/2} |b_j|.$$

225 Since $k_{F_1}^{-1} = k_1^{-1} + k_2^{-1}$, we clearly have $k_{F_1}^{-1/2} k_j^{1/2} \leq 2\mathcal{C}_N$, which yields (4.9) for $i = 1$.
226 Using now the expression of x_i for $i \geq 2$ from (4.7) we obtain:

$$k_{F_i}^{-1/2} |x_i| \leq \sum_{j=2}^i \frac{\bar{\Lambda}_j}{\Lambda_1} k_{F_i}^{-1/2} |b_j| + \sum_{j=i+1}^{n_N} \frac{\Lambda_j}{\Lambda_1} k_{F_i}^{-1/2} |b_j|, \quad 2 \leq i \leq n_N - 1 \quad (4.10)$$

$$k_{F_{n_N}}^{-1/2} |x_{n_N}| \leq \sum_{j=2}^{n_N} \frac{\bar{\Lambda}_j}{\Lambda_1} k_{F_i}^{-1/2} |b_j|. \quad (4.11)$$

227 The second sum in (4.10) is bounded similarly to the case of x_1 . We use $0 < \frac{\Lambda_j}{\Lambda_1} \leq 1$

228 and $k_{F_i}^{-1} = k_i^{-1} + k_{i+1}^{-1}$ and we thus get:

$$\sum_{j=i+1}^{n_N} \frac{\Lambda_j}{\Lambda_1} k_{F_i}^{-1/2} |b_j| \leq \sum_{j=i+1}^{n_N} (k_{F_i}^{-1/2} k_j^{1/2}) k_j^{-1/2} |b_j| \leq 2\mathcal{C}_N \sum_{j=i+1}^{n_N} k_j^{-1/2} |b_j|. \quad (4.12)$$

As regards the first sum in (4.10) and in (4.11), we first use that $\Lambda_1 \geq k_{F_i}^{-1} + k_{F_l}^{-1}$ for any indices i, l in order to obtain, for any index j such that $2 \leq j \leq i$,

$$\frac{\bar{\Lambda}_j}{\Lambda_1} k_{F_i}^{-1/2} |b_j| = \left(\sum_{l=1}^{j-1} k_{F_l}^{-1} \right) \frac{k_{F_i}^{-1/2}}{\Lambda_1} |b_j| = \sum_{l=1}^{j-1} \frac{k_{F_l}^{-1} k_{F_i}^{-1/2}}{\Lambda_1} |b_j| \leq \sum_{l=1}^{j-1} k_{F_l}^{-1/2} \frac{k_{F_l}^{-1/2} k_{F_i}^{-1/2}}{k_{F_l}^{-1} + k_{F_i}^{-1}} |b_j|.$$

Thanks to the mean inequality, we further get

$$\frac{\bar{\Lambda}_j}{\Lambda_1} k_{F_i}^{-1/2} |b_j| \leq \frac{1}{2} \sum_{l=1}^{j-1} k_{F_l}^{-1/2} |b_j| = \frac{1}{2} \left(\sum_{l=1}^{j-1} k_{F_l}^{-1/2} k_j^{1/2} \right) k_j^{-1/2} |b_j|.$$

Since $l+1 \leq j$, the same argument as above, namely $k_{F_l}^{-1/2} k_j^{1/2} \leq 2\mathcal{C}_N$, yields that

$$\frac{\bar{\Lambda}_j}{\Lambda_1} k_{F_i}^{-1/2} |b_j| \leq (j-1) \mathcal{C}_N k_j^{-1/2} |b_j|, \quad 2 \leq j \leq i.$$

229 Since n_N is uniformly bounded, we next get:

$$\sum_{j=2}^i \frac{\bar{\Lambda}_j}{\Lambda_1} k_{F_i}^{-1/2} |b_j| \lesssim \mathcal{C}_N \sum_{j=2}^i k_j^{-1/2} |b_j|. \quad (4.13)$$

230 Finally, using (4.12) and (4.13) in (4.10) yields the result for $2 \leq i \leq n_N$. \square

We can now deduce the next bound for θ_N , with respect to the local norm

$$\|\mu_h\|_{\mathcal{F}_N}^2 := \sum_{F \in \mathcal{F}_N \cap \mathcal{F}_h^{int}} \int_F |F| k_F^{-1} \mu_h^2 ds, \quad \mu_h \in \mathcal{M}_h.$$

231

232

LEMMA 4.3. *For any $N \in \mathcal{N}_h$, one has that:*

$$\|\theta_N\|_{\mathcal{F}_N} \lesssim \mathcal{C}_N \sum_{T \in \omega_N} k_T^{-1/2} |r_h(\varphi_N \chi_T)|. \quad (4.14)$$

233

234

235

236

Proof. The definition of θ_N yields that $\|\theta_N\|_{\mathcal{F}_N}^2 = \frac{1}{3} \sum_{i=1}^{m_N} k_{F_i}^{-1} x_i^2$, with $m_N := n_N$ if $N \in \mathcal{N}_h^{int}$ and $m_N := n_N - 1$ if $N \in \mathcal{N}_h^\partial$. The result follows from Lemma 4.2. \square

We are now able to prove the main result of this section. For $l \in \mathbb{N}$, we denote by π_ω^l the $L^2(\omega)$ -orthogonal projection on $P^l(\omega)$.

THEOREM 4.4. *For any $N \in \mathcal{N}_h$, the local multiplier satisfies the bound:*

$$\begin{aligned} \|\theta_N\|_{\mathcal{F}_N} &\lesssim \mathcal{C}_N \sum_{T \in \omega_N} \left(\frac{h_T}{k_T^{1/2}} \|\pi_T^1 f\|_{0,T} + \sum_{F \in \partial T \cap \mathcal{F}_h^{int}} \frac{\bar{\omega}_{F,T} h_F^{1/2}}{k_T^{1/2}} \|[K \nabla u_h \cdot n_F]\|_{0,F \cap \mathcal{F}_N} \right. \\ &+ \left. \sum_{F \in \partial T \cap \Gamma_D} \frac{k_F^{1/2}}{h_F^{1/2}} \|u_h - \pi_F^1 g_D\|_{0,F \cap \mathcal{F}_N} + \sum_{F \in \partial T \cap \Gamma_N} \frac{h_F^{1/2}}{k_F^{1/2}} \|K \nabla u_h \cdot n - \pi_F^1 g_N\|_{0,F \cap \mathcal{F}_N} \right) \end{aligned}$$

237

where $\bar{\omega}_{F,T} = \omega_F^\pm$ if $T = T^\mp$ with respect to n_F .

Proof. Let any $T \in \omega_N$. Using that $[u_h]_F = 0$ for any $F \in \mathcal{F}_h^{int}$, we have that:

$$\begin{aligned} r_h(\varphi_N \chi_T) &= l_h(\varphi_N \chi_T) - \tilde{a}_h(u_h, \varphi_N \chi_T) \\ &= \int_T f \varphi_N dx + \int_{\partial T \cap \Gamma_N} g_N \varphi_N ds - \int_{\partial T \cap \Gamma_D} K \nabla \varphi_N \cdot n (g_D - u_h) ds \\ &\quad + \int_{\partial T \cap \Gamma_D} \frac{\gamma k_F}{|F|} \varphi_N (g_D - u_h) ds - \int_T K \nabla u_h \cdot \nabla \varphi_N dx \\ &\quad + \int_{\partial T \cap \Gamma_D} K \nabla u_h \cdot n \varphi_N ds + \int_{\partial T \cap \mathcal{F}_h^{int}} \{K \nabla u_h \cdot n_F\} [\varphi_N \chi_T] ds. \end{aligned}$$

Thanks to integration by parts and to the well-known formula $[ab] = \{a\}[b] + [a]\{b\}^*$, we obtain, since $K \nabla u_h$ is constant on T , that

$$\begin{aligned} r_h(\varphi_N \chi_T) &= \int_T f \varphi_N dx + \int_{\partial T \cap \Gamma_N} (g_N - K \nabla u_h \cdot n) \varphi_N + \int_{\partial T \cap \Gamma_D} \frac{\gamma k_F}{|F|} \varphi_N (g_D - u_h) \\ &\quad - \int_{\partial T \cap \Gamma_D} K \nabla \varphi_N \cdot n (g_D - u_h) ds - \int_{\partial T \cap \mathcal{F}_h^{int}} [K \nabla u_h \cdot n_F] \{\varphi_N \chi_T\}^* ds. \end{aligned}$$

Noting that φ_N vanishes on $\mathcal{F}_h \setminus \mathcal{F}_N$, a standard scaling argument yields that:

$$\begin{aligned} |r_h(\varphi_N \chi_T)| &\lesssim h_T \|\pi_T^1 f\|_{0,T} + \sum_{F \in \partial T \cap \mathcal{F}_N \cap \Gamma_N} h_F^{1/2} \|K \nabla u_h \cdot n - \pi_F^1 g_N\|_{0,F} \\ &+ \sum_{F \in \partial T \cap \mathcal{F}_N \cap \Gamma_D} \frac{\gamma k_F}{h_F^{1/2}} \|u_h - \pi_F^1 g_D\|_{0,F} + \sum_{F \in \partial T \cap \Gamma_D} \frac{k_T}{h_F^{1/2}} \|\pi_F^0(u_h - g_D)\|_{0,F} \\ &+ \sum_{F \in \partial T \cap \mathcal{F}_N \cap \mathcal{F}_h^{int}} h_F^{1/2} \bar{\omega}_{F,T} \|[K \nabla u_h \cdot n_F]\|_{0,F}. \end{aligned}$$

238 We next multiply the previous inequality by $k_T^{-1/2}$ and use that $k_F = k_T$ on the
239 Dirichlet sides, and that $\|\pi_F^0 w\|_{0,F} \leq \|\pi_F^1 w\|_{0,F}$. Lemma 4.3 yields the result. \square

4.2. Nonconforming approximation. The residual is now given by:

$$r_h^*(\cdot) = l_h(\cdot) - \tilde{a}_h^*(u_h, \cdot).$$

240 Thanks to the mixed formulation, we have $r_h^*(v_h) = 0$ for any $v_h \in \mathcal{NC}_h^k$ and

$$l_h^*(\theta_h^*, v_h) = r_h^*(v_h) \quad \forall v_h \in \mathcal{DG}_h^k. \quad (4.15)$$

241 Let any $F \in \mathcal{F}_h^{int}$. We define $\theta_F \in \mathcal{M}_h^{k-1}$ by imposing $(\theta_F)_{|F'} = 0$ for any
242 $F' \neq F$, whereas $(\theta_F)_{|F} \in P^{k-1}$ is given by:

$$b_h^*(\theta_F, \phi_{F,i} \chi_T) = r_h^*(\phi_{F,i} \chi_T), \quad \forall T \in \Delta_F, \quad 0 \leq i \leq k-1. \quad (4.16)$$

The support of $\phi_{F,i} \in \mathcal{NC}_h^k$ is Δ_F so we have that

$$0 = r_h^*(\phi_{F,i}) = \sum_{T \in \Delta_F} r_h^*(\phi_{F,i} \chi_T), \quad 0 \leq i \leq k-1.$$

Furthermore, by definition of the nonconforming space, we also have that

$$\sum_{T \in \Delta_F} b_h^*(\theta_F, \phi_{F,i} \chi_T) = \int_F \theta_F [\phi_{F,i}] ds = 0, \quad 0 \leq i \leq k-1.$$

243 So the system (4.16) is compatible and is equivalent to:

$$\int_F \theta_F \phi_{F,i} ds = \mathfrak{s}_{F,T^*} r_h^*(\phi_{F,i} \chi_{T^*}), \quad 0 \leq i \leq k-1 \quad (4.17)$$

244 where T^* is the triangle of Δ_F with the smallest coefficient k and $\mathfrak{s}_{F,T^*} = n_F \cdot n_{T^*}$.
245 Writing $\theta_F \in P^{k-1}(F)$ in the Legendre basis as $\theta_F = \sum_{j=0}^{k-1} \theta_{F,j} L_j$ yields the unique
246 solution of (4.17), with $|F| |\theta_{F,j}| = |r_h^*(\phi_{F,j} \chi_{T^*})|$ for $0 \leq j \leq k-1$. In addition, using
247 that $k_F^{-1} \leq 2k_{T^*}^{-1}$ we get a robust bound for θ_F , similar to the one of Lemma 4.3:

$$\|\theta_F\|_{\mathcal{NC}_h}^2 \lesssim k_F^{-1} |F|^2 \sum_{j=0}^{k-1} \theta_{F,j}^2 \leq 2k_{T^*}^{-1} \sum_{j=0}^{k-1} r_h^*(\phi_{F,j} \chi_{T^*})^2. \quad (4.18)$$

248 **LEMMA 4.5.** *Let θ_h^* and θ_F be the solutions of (4.15) and (4.16), respectively.*

249 *Then $\theta_h^* = \sum_{F \in \mathcal{F}_h^{int}} \theta_F$.*

250 *Proof.* Let $\bar{\theta}_h := \sum_{F \in \mathcal{F}_h^{int}} \theta_F$. We show that $\bar{\theta}_h$ satisfies (4.15), which yields that

251 $\bar{\theta}_h = \theta_h^*$ thanks to the inf-sup condition.

We first consider $v_h = \phi_j^T \chi_T$, for any $T \in \mathcal{T}_h$ and $0 \leq j \leq \frac{k(k-1)}{2}$. On the one hand, since this test-function belongs to \mathcal{NC}_h^k , we have that $r_h^*(\phi_j^T \chi_T) = 0$. On the other hand, we also have

$$b_h^*(\bar{\theta}_h, \phi_j^T \chi_T) = \sum_{F \in \mathcal{F}_h^{int}} b_h^*(\theta_F, \phi_j^T \chi_T) = \sum_{F \in (\partial T \cap \mathcal{F}_h^{int})} \mathfrak{s}_{F,T} \int_F \theta_F \phi_j^T ds = 0,$$

252 by using the decomposition of θ_F in the Legendre basis of $P^{k-1}(F)$ and the degrees
253 of freedom (3.5) of the nodal basis function ϕ_j^T .

Next, we take $v_h = \phi_{F,i} \chi_T$, for any $F \in \mathcal{F}_h$, $T \subset \Delta_F$ and $0 \leq i \leq k-1$. If $F \in \mathcal{F}_h^{int}$, then we have thanks to (4.16):

$$b_h^*(\bar{\theta}_h, \phi_{F,i} \chi_T) = \sum_{F' \in \mathcal{F}_h^{int}} b_h^*(\theta_{F'}, \phi_{F,i} \chi_T) = b_h^*(\theta_F, \phi_{F,i} \chi_T) = r_h^*(\phi_{F,i} \chi_T).$$

254 Here above, we have used the fact that $\int_{F'} \theta_{F'} \phi_{F,i} ds = 0$ for $F' \neq F$, according to
255 (3.5). Finally, if $F \in \mathcal{F}_h^{\partial}$ then $v_h \in \mathcal{NC}_h^k$ so $r_h^*(v_h) = 0$, and $b_h^*(\bar{\theta}_h, v_h) = 0$ too.

256 We have thus shown that $b_h^*(\bar{\theta}_h, v_h) = r_h^*(v_h)$ for any $v_h \in \mathcal{DG}_h^k$, so $\bar{\theta}_h = \theta_h^*$. \square

257 5. Local flux reconstruction.

258 **5.1. Conforming approximation.** Thanks to the definition of the multiplier
259 θ_h , we are now able to reconstruct the local flux σ_h belonging to $H(\text{div}, \Omega)$. For this
260 purpose, we use the Raviart-Thomas finite element space RT_h^m , with $m = 0$ or 1 . We
261 impose the degrees of freedom of σ_h as follows.

262 On the Neumann boundary, we simply set on any $F \in \mathcal{F}_h^N$:

$$\sigma_h \cdot n_F = \pi_h^m g_N. \quad (5.1)$$

263 On the Dirichlet boundary, we set on any $F \in \mathcal{F}_h^D$:

$$\int_F \sigma_h \cdot n_F \varphi ds = \int_F \left(K \nabla u_h \cdot n_F - \frac{\gamma k_F}{|F|} (u_h - g_D) \right) \varphi ds, \quad \forall \varphi \in P^m(F), \quad (5.2)$$

264 which translates into $\sigma_h \cdot n_F = K \nabla u_h \cdot n_F - \frac{\gamma k_F}{|F|} \pi_F^m (u_h - g_D)$. On a interior side

265 $F \in \mathcal{F}_h^{int}$ we impose:

$$\int_F \sigma_h \cdot n_F \varphi ds = \int_F \{K \nabla u_h \cdot n_F\} \varphi ds - b_F(\theta_h, \varphi), \quad \forall \varphi \in P^m(F). \quad (5.3)$$

266 The previous relations allow to uniquely define $\sigma_h \cdot n_F$ in $P^m(F)$ for any $F \in \mathcal{F}_h$.

267 If $m = 1$, then we also define interior degrees of freedom on any $T \in \mathcal{T}_h$ as follows:

$$\int_T \sigma_h \cdot r dx = \int_T K \nabla u_h \cdot r dx - \int_{\partial T \cap \Gamma_D} (u_h - g_D) K r \cdot n ds, \quad \forall r \in (P^0(T))^2. \quad (5.4)$$

268 Similarly to [10], we can then prove the following statement.

269 **THEOREM 5.1.** *The flux σ_h satisfies the following conservation property:*

$$(\text{div } \sigma_h)|_T = -\pi_T^m f, \quad \forall T \in \mathcal{T}_h. \quad (5.5)$$

270 **5.2. Nonconforming approximation.** We are now able to reconstruct the
 271 local flux σ_h^* in $H(\text{div}, \Omega)$, more precisely in the Raviart-Thomas finite element space
 272 RT_h^{k-1} . On the sides, its degrees of freedom are given by:

$$\begin{aligned} \forall F \in \mathcal{F}_h^N, \quad \sigma_h^* \cdot n_F &= \pi_F^{k-1} g_N, \\ \forall F \in \mathcal{F}_h^D, \quad \sigma_h^* \cdot n_F &= \pi_F^{k-1} \left(K \nabla u_h^* \cdot n_F - \frac{\gamma^{k_F}}{|F|} (u_h^* - g_D) \right), \\ \forall F \in \mathcal{F}_h^{\text{int}}, \quad \sigma_h^* \cdot n_F &= \pi_F^{k-1} \{ K \nabla u_h^* \cdot n_F \} - \theta_h^*. \end{aligned} \quad (5.6)$$

273 The interior degrees of freedom are defined as follows, for any $T \in \mathcal{T}_h$, $r \in (P^{k-2}(T))^2$:

$$\int_T \sigma_h^* \cdot r \, dx = \int_T K \nabla u_h^* \cdot r \, dx - \int_{\partial T \cap \mathcal{F}_h^D} (u_h^* - g_D) K r \cdot n \, ds, \quad \forall r \in (P^{k-2}(T))^2. \quad (5.7)$$

274

THEOREM 5.2. *The flux σ_h^* satisfies the following conservation property:*

$$(\text{div} \sigma_h^*)|_T = -\pi_T^{k-1} f, \quad \forall T \in \mathcal{T}_h.$$

275 *Proof.* Let $T \in \mathcal{T}_h$, $p \in P^{k-1}(T) \subset V_k(T)$ and let $v := p \chi_T \in \mathcal{DG}_h^k$. We start from
 276 the integration by parts formula:

$$- \int_T (\text{div} \sigma_h^*) p \, dx = \int_T \sigma_h^* \cdot \nabla v \, dx - \int_{\partial T} \sigma_h^* \cdot n_T v \, ds. \quad (5.8)$$

From (5.6) and (5.7) with $r := \nabla v$, we get using $v|_F n_T = [v]_F n_F$ that:

$$\begin{aligned} \int_F \sigma_h^* \cdot n_T v \, ds &= \int_F \{ K \nabla u_h^* \cdot n_F \} [v] \, ds - \int_F \theta_h^* [v] \, ds, \quad \forall F \in \partial T \cap \mathcal{F}_h^{\text{int}}, \\ \int_F \sigma_h^* \cdot n_T v \, ds &= \int_F K \nabla u_h^* \cdot n_F v \, ds - \int_F \frac{\gamma^{k_F}}{|F|} (u_h^* - g_D) v \, ds, \quad \forall F \in \partial T \cap \mathcal{F}_h^D, \\ \int_F \sigma_h^* \cdot n_T v \, ds &= \int_F g_N v \, ds, \quad \forall F \in \partial T \cap \mathcal{F}_h^N, \\ \int_T \sigma_h^* \cdot \nabla v \, dx &= \int_T K \nabla u_h^* \cdot \nabla v \, dx - \int_{\partial T \cap \mathcal{F}_h^D} (u_h^* - g_D) K \nabla v \cdot n \, ds. \end{aligned}$$

Replacing in (5.8) we obtain:

$$\begin{aligned} - \int_T (\text{div} \sigma_h^*) p \, dx &= \int_T K \nabla u_h^* \cdot \nabla v \, dx - \int_{\partial T \cap \mathcal{F}_h^D} (K \nabla v \cdot n u_h^* + K \nabla u_h^* \cdot n v) \, ds \\ &\quad + \int_{\partial T \cap \mathcal{F}_h^D} \frac{\gamma^{k_F}}{|F|} (u_h^* - g_D) v \, ds - \int_{\partial T \cap \mathcal{F}_h^{\text{int}}} \pi_F^{k-1} \{ K \nabla u_h^* \cdot n_F \} [v] \, ds \\ &\quad + \sum_{F \in \partial T \cap \mathcal{F}_h^{\text{int}}} \int_F \theta_h^* [v] \, ds + \int_{\partial T \cap \mathcal{F}_h^D} g_D K \nabla v \cdot n \, ds - \int_{\partial T \cap \mathcal{F}_h^N} g_N v \, ds. \end{aligned}$$

Noting that $\int_{\partial T \cap \mathcal{F}_h^{\text{int}}} \pi_F^{k-1} \{ K \nabla v \cdot n_F \} [u_h^*] \, ds = 0$ because $u_h^* \in \mathcal{NC}_h^k$, we further get

$$- \int_T (\text{div} \sigma_h^*) p \, dx = \tilde{a}_h^*(u_h^*, v) + b_h^*(\theta_h^*, v) - l_h(v) + \int_T f v \, dx = \int_T f p \, dx,$$

277 since (u_h^*, θ_h^*) is solution of the mixed formulation (3.2). This ends the proof. \square

6. Application to a posteriori error analysis. We only consider here the P^1 -continuous approximation. For the sake of simplicity, we set $f_h = \pi_T^m f$ and $g_h = \pi_F^m g_N$, and we also assume that g_D is a piecewise P^1 -continuous function. Let $\tau_h = K^{-1/2}(\sigma_h - K\nabla u_h)$. We introduce the local error estimators:

$$\begin{aligned}\eta_T &= \|K^{-1/2}(\sigma_h - K\nabla u_h)\|_{0,T} = \|\tau_h\|_{0,T}, \quad \forall T \in \mathcal{T}_h, \\ \eta_F &= \left(\int_F \frac{k_F}{|F|} (u_h - g_D)^2 ds \right)^{1/2}, \quad \forall F \in \mathcal{F}_h^D,\end{aligned}$$

and the corresponding global error estimators

$$\eta = \left(\sum_{T \in \mathcal{T}_h} \eta_T^2 \right)^{1/2} = \|\tau_h\|_{0,\Omega}, \quad \eta_D = \left(\sum_{F \in \mathcal{F}_h^D} \eta_F^2 \right)^{1/2}.$$

Let also the following higher order term, representing the data approximation:

$$\epsilon(\Omega)^2 = \sum_{T \in \mathcal{T}_h} \frac{h_T^2}{k_T} \|f - f_h\|_{0,T}^2 + \sum_{F \in \mathcal{F}_h^N} \frac{h_F}{k_F} \|g_N - g_h\|_{0,F}^2.$$

278 **6.1. Reliability.** LEMMA 6.1. *Let σ_h be given by the equations (5.1)-(5.4)*
 279 *and let u_h the solution of the weak formulation (3.1). Then we have the following*
 280 *estimate:*

$$|u - u_h|_{1,K} \leq \eta + C_D \eta_D + C\epsilon(\Omega) \quad (6.1)$$

281 where $C_D \simeq \max_{N \in \mathcal{N}_h^D} \{C_N\}$ and C_N is defined in (4.5).

282 *Proof.* Let $\varphi \in V^{g_D}$ the unique solution of

$$\int_{\Omega} K\nabla\varphi \cdot \nabla v \, dx = \int_{\Omega} K\nabla u_h \cdot \nabla v \, dx, \quad \forall v \in V^0. \quad (6.2)$$

283 By the triangle inequality, we have

$$|u - u_h|_{1,K} \leq |u - \varphi|_{1,K} + |\varphi - u_h|_{1,K}, \quad (6.3)$$

where

$$\begin{aligned}|u - \varphi|_{1,K}^2 &= \int_{\Omega} K^{1/2} \nabla(u - \varphi) \cdot (K^{1/2} \nabla u - K^{-1/2} \sigma_h) \, dx \\ &\quad + \int_{\Omega} K^{1/2} \nabla(u - \varphi) \cdot \tau_h \, dx + \int_{\Omega} K^{1/2} \nabla(u - \varphi) \cdot K^{1/2} \nabla(u_h - \varphi) \, dx \\ &\leq |u - \varphi|_{1,K} \|\tau_h\|_{\Omega} + \int_{\Omega} \nabla(u - \varphi) \cdot (K\nabla u - \sigma_h) \, dx,\end{aligned}$$

by testing (6.2) with $v := u - \varphi \in V^0$. Since $K\nabla u - \sigma_h \in H(\text{div}, \Omega)$ and $u - \varphi \in H^1(\Omega)$, integration by parts in the last term yields, thanks to Lemma 5.1, that:

$$\int_{\Omega} \nabla(u - \varphi) \cdot (K\nabla u - \sigma_h) \, dx = \int_{\Omega} (f - f_h)(u - \varphi) \, dx + \int_{\Gamma_N} (g_N - g_h)(u - \varphi) \, ds.$$

The right-hand side term is classically bounded by $C|u - \varphi|_{1,K}\epsilon(\Omega)$. Thus, we have so far proved that

$$|u - \varphi|_{1,K} \leq \eta + C\epsilon(\Omega).$$

We next bound the remaining term in (6.3), $|u_h - \varphi|_{1,K}$. From (6.2), we have

$$|\varphi - u_h|_{1,K} = \inf_{v \in V^{g_D}} |v - u_h|_{1,K}$$

so it is sufficient to build $v \in V^{g_D}$ such that $|v - u_h|_{1,K}$ is bounded by η_D . We choose $v \in \mathcal{C}_h^1$ defined by

$$v(N) = u_h(N), \quad \forall N \in \mathcal{N}_h^{int} \cup \mathcal{N}_h^N, \quad v(N) = g_D(N) \quad \forall N \in \mathcal{N}_h^D.$$

For simplicity of notation, we set $\mathcal{D} = \{T \in \mathcal{T}_h : T \cap \bar{\Gamma}_D \neq \emptyset\}$. Then we have

$$|v - u_h|_{1,K}^2 = \sum_{T \in \mathcal{D}} \int_T K \nabla(v - u_h) \cdot \nabla(v - u_h) dx \lesssim \sum_{T \in \mathcal{D}} \sum_{N \in \mathcal{N}_T} k_T (v - u_h)^2(N).$$

For a triangle $T \in \mathcal{D}$ which has a side $F \in \mathcal{F}_h^D$, one has that $k_F = k_T$ and

$$\sum_{N \in \mathcal{N}_T} k_T (v - u_h)(N)^2 = \sum_{N \in \mathcal{N}_F} k_F (g_D - u_h)^2(N) \simeq \eta_F^2.$$

Meanwhile, for $T \in \mathcal{D}$ which has only a node $N \in \mathcal{N}_h^D$, one can bound k_T by $\mathcal{C}_N^2 k_F$, where $F \in \mathcal{F}_h^D \cap \mathcal{F}_N$. Hence, we finally get that

$$|v - u_h|_{1,K} \leq \mathcal{C}_D \eta_D$$

284 and the announced bound follows from (6.3). \square

285 **REMARK 1.** For $m = 1$, the definition of σ_h on a Dirichlet side $F \subset \partial T$ together
286 with the Cauchy-Schwarz inequality yield that $\eta_F \leq h_F^{1/2} \gamma^{-1} \|\tau_h \cdot n\|_{0,F} \lesssim \gamma^{-1} \|\tau_h\|_{0,T}$,
287 so one can bound η_D by η .

6.2. Efficiency. LEMMA 6.2. Let $T \in \mathcal{T}_h$. We have the following estimate:

$$\begin{aligned} \eta_T &\lesssim \mathcal{C}_T \sum_{T' \in \Delta_T} \left(\frac{h_{T'}}{k_{T'}^{1/2}} \|f_h\|_{0,T'} + \sum_{F \in \partial T' \cap \Gamma_D} \frac{k_F^{1/2}}{h_F^{1/2}} \|u_h - g_D\|_{0,F} \right. \\ &\quad \left. + \sum_{F \in \partial T' \setminus \partial \Delta_T} \frac{\bar{\omega}_{F,T'} h_F^{1/2}}{k_{T'}^{1/2}} \|[K \nabla u_h \cdot n_F]\|_{0,F} \right) + \sum_{F \in \partial T \cap \Gamma_N} \frac{h_F^{1/2}}{k_T^{1/2}} \|K \nabla u_h \cdot n - g_h\|_{0,F} \end{aligned}$$

288 where $\mathcal{C}_T = \max_{N \in \mathcal{N}_T} \mathcal{C}_N$ and $\Delta_T = \{T' \in \mathcal{T}_h; \partial T' \cap \partial T \neq \emptyset\}$.

289 *Proof.* Using the degrees of freedom of the Raviart-Thomas space $RT^m(T)$, we
290 have the following well-known inequality for $\tau_h = K^{-1/2}(\sigma_h - K \nabla u_h)$:

$$\|\tau_h\|_{0,T} \lesssim \frac{1}{k_T^{1/2}} \|\pi_T^{m-1}(\sigma_h - K_T \nabla u_h)\|_{0,T} + \sum_{F \in \partial T} \frac{h_F^{1/2}}{k_T^{1/2}} \|(\sigma_h - K_T \nabla u_h) \cdot n_F\|_{0,F}. \quad (6.4)$$

291 We next bound the right-hand-side term using the definition of the flux, that is
292 relations (5.1)-(5.4). For $F \in \partial T \cap \Gamma_N$, we immediately have that:

$$h_F^{1/2} k_T^{-1/2} \|(\sigma_h - K_T \nabla u_h) \cdot n_F\|_{0,F} = h_F^{1/2} k_T^{-1/2} \|K_T \nabla u_h \cdot n - g_h\|_{0,F}, \quad (6.5)$$

293 whereas for $F \in \partial T \cap \Gamma_D$ we have with $k_F = k_T$:

$$h_F^{1/2} k_T^{-1/2} \|(\sigma_h - K_T \nabla u_h) \cdot n_F\|_{0,F} = \gamma h_F^{-1/2} k_F^{1/2} \|\pi_F^m(u_h - g_D)\|_{0,F}. \quad (6.6)$$

For $F \in \partial T \cap \mathcal{F}_h^{int}$, we use that $\{a\} - a^- = -\omega^+[a]$ and $\{a\} - a^+ = \omega^-[a]$ and we get, for any $\varphi \in P^m(F)$:

$$\int_F (\sigma_h - K_T \nabla u_h) \cdot n_F \varphi \, ds = -(n_F \cdot n_T) \bar{\omega}_{F,T} \int_F [K \nabla u_h \cdot n_F] \varphi \, ds - b_F(\theta_h, \varphi).$$

Taking $\varphi = (\sigma_h - K_T \nabla u_h) \cdot n_F$ as test-function and using that $k_F \leq k_T$, we get

$$\begin{aligned} h_F^{1/2} k_T^{-1/2} \|(\sigma_h - K_T \nabla u_h) \cdot n_F\|_{0,F} &\lesssim h_F^{1/2} k_T^{-1/2} \bar{\omega}_{F,T} \| [K \nabla u_h \cdot n_F] \|_{0,F} \\ &\quad + \left(\sum_{N \in \mathcal{N}_F} |F| k_F^{-1} (\theta_N)_{|F}^2(N) \right)^{1/2}. \end{aligned}$$

294 Let $\mathcal{D}_F = \bigcup_{N \in \mathcal{N}_F} \omega_N = \{T' \in \mathcal{T}_h; \partial T' \cap \bar{F} \neq \emptyset\}$ and $\mathcal{C}_F = \max_{N \in \mathcal{N}_F} \mathcal{C}_N$. Thanks to

295 Theorem 4.4, we deduce that:

$$\begin{aligned} &h_F^{1/2} k_T^{-1/2} \|(\sigma_h - K \nabla u_h) \cdot n_F\|_{0,F} \\ &\lesssim \mathcal{C}_F \sum_{T' \in \mathcal{D}_F} \left(\frac{h_{T'}}{k_{T'}^{1/2}} \|f_h\|_{0,T'} + \sum_{F' \in \partial T' \setminus \partial \mathcal{D}_F} \frac{\bar{\omega}_{F',T'} h_{F'}^{1/2}}{k_{T'}^{1/2}} \| [K \nabla u_h \cdot n_{F'}] \|_{0,F'} \right. \\ &\quad \left. + \sum_{F' \in \partial T' \cap \Gamma_N} \frac{h_{F'}^{1/2}}{k_{T'}^{1/2}} \|K_{T'} \nabla u_h \cdot n - g_h\|_{0,F'} + \sum_{F' \in \partial T' \cap \Gamma_D} \frac{k_{F'}^{1/2}}{h_{F'}^{1/2}} \|u_h - g_D\|_{0,F'} \right). \end{aligned} \quad (6.7)$$

296 Concerning the interior degrees of freedom (for $m = 1$), taking $r = \pi_T^0(\sigma_h - K_T \nabla u_h)$
297 in (5.4) yields that

$$k_T^{-1/2} \|\pi_T^0(\sigma_h - K \nabla u_h)\|_{0,T} \lesssim \sum_{F \in \partial T \cap \Gamma_D} h_F^{-1/2} k_F^{1/2} \|\pi_F^0(u_h - g_D)\|_{0,F}. \quad (6.8)$$

Gathering together (6.5), (6.6), (6.7) and (6.8) in (6.4) and putting

$$\mathcal{C}_T := \max_{F \in \partial T} \mathcal{C}_F = \max_{N \in \mathcal{N}_T} \mathcal{C}_N, \quad \Delta_T := \bigcup_{F \in \partial T \cap \mathcal{F}_h^{int}} \mathcal{D}_F = \{T' \in \mathcal{T}_h; \partial T' \cap \partial T \neq \emptyset\},$$

298 we obtain the desired bound. \square

299 For any $T \in \mathcal{T}_h$ and $F \in \partial T \cap \mathcal{F}_h^N$, we have thanks to Verfurth's argument [24]:

$$\begin{aligned} \frac{h_T}{k_T^{1/2}} \|f_h\|_{0,T} &\lesssim |u - u_h|_{1,T,K} + \frac{h_T}{k_T^{1/2}} \|f - f_h\|_{0,T}, \\ \frac{h_F^{1/2}}{k_F^{1/2}} \|K \nabla u_h \cdot n - g_h\|_{0,F} &\lesssim |u - u_h|_{1,T,K} + \frac{h_T}{k_T^{1/2}} \|f - f_h\|_{0,T} + \frac{h_F^{1/2}}{k_F^{1/2}} \|g_N - g_h\|_{0,F}. \end{aligned} \quad (6.9)$$

LEMMA 6.3. *Let $T \in \mathcal{T}_h$ and $F \in \partial T \cap \mathcal{F}_h^{int}$. Then we have:*

$$\frac{h_F^{1/2} \bar{\omega}_{F,T}}{k_T^{1/2}} \| [K \nabla u_h \cdot n_F] \|_{0,F} \lesssim |u - u_h|_{1,\Delta_F,K} + \sum_{T' \subset \Delta_F} \frac{h_{T'}}{k_{T'}^{1/2}} \|f - f_h\|_{0,T'}.$$

Proof. We start from the next estimate, obtained again by means of Verfurth's argument:

$$h_F^{1/2} \|[K\nabla u_h \cdot n_F]\|_{0,F} \lesssim \sum_{T' \subset \Delta_F} \|K\nabla(u - u_h)\|_{0,T'} + \sum_{T' \subset \Delta_F} h_{T'} \|f - f_h\|_{0,T'}.$$

We multiply the inequality by $\bar{\omega}_{F,T} k_T^{-1/2}$ and we note that for $T' = T$, we obviously have $(\bar{\omega}_{F,T} k_{T'}^{1/2}) k_T^{-1/2} = \bar{\omega}_{F,T} \leq 1$, whereas for $T' \neq T$ we get, thanks to the definition of $\bar{\omega}_{F,T}$ and to the mean inequality,

$$\frac{\bar{\omega}_{F,T} k_{T'}^{1/2}}{k_T^{1/2}} = \frac{k_T^{1/2} k_{T'}^{1/2}}{k_T + k_{T'}} \leq \frac{1}{2}.$$

300 This finally yields the announced estimate. \square

301 Combining Lemmas 6.2 and 6.3 and estimates (6.9), we have the following result.

THEOREM 6.4 (Efficiency). *We have the following local efficiency bound:*

$$\eta_T \lesssim \mathcal{C}_T (\|u - u_h\|_{\Delta_T} + \epsilon(\Delta_T)),$$

302 with $\mathcal{C}_T = 1$ if the coefficient K is quasi-monotone.

303 Note that by definition of the energy norm, one also has that $\eta_F \leq \|u - u_h\|_{\Delta_F}$
304 for any Dirichlet side F .

305 **7. Numerical tests.** We present some numerical experiments carried out for the
306 P^1 -continuous approximation. For the stabilisation parameter in Nitsche's method,
307 we set $\gamma = 50$. As regards the refinement strategy, we use the Dörfler marking strategy
308 and the refinement rate is set to be 10%. In the adaptive mesh refinement (AMR)
309 procedure, the marking percent is set to be 20%.

EXAMPLE 7.1 (The Ellipse Example). *Let $\Omega = [-1, 1]^2$ and let the ellipse centered at the origin, with width $2a$ and height $2b$, of equation $\rho = 1$, where $\rho = \sqrt{\frac{x^2}{a^2} + \frac{y^2}{b^2}}$. Here, we take $a = \frac{\pi}{6.18}$ and $b = 1.5a$. The exact solution is given by*

$$u(x, y) = \begin{cases} \frac{1}{k_1} \rho^p & \text{if } \rho \leq 1 \\ \frac{1}{k_2} \rho^p + \frac{1}{k_1} - \frac{1}{k_2} & \text{if } \rho > 1 \end{cases},$$

310 where $p = 5$ and the diffusion coefficients in the two sub-domains are $k_1 = 1.0$ and
311 $k_2 = 10k_1$, respectively.

312 The stopping criteria in the AMR procedure is that the total number N of degrees
313 of freedom is less than 15000. The initial and final mesh generated by η_K are provided
314 in Figure 7.1.

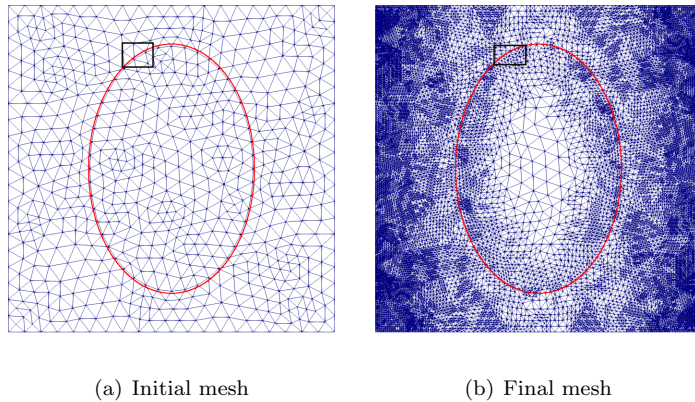


Fig. 7.1: (Example 7.1) Initial and final meshes

315 In Figure 7.2, we show the process of boundary snapping. When an element is
 316 refined, we use the longest edge refinement method, i.e., we add the mid-point of the
 317 longest edge to the vertices and form two sub-triangles. If the longest edge has two
 318 endpoints lying on the interface, we will adjust the newly added vertex to the interface
 319 after the refinement if such a movement does not deteriorate the mesh regularity.

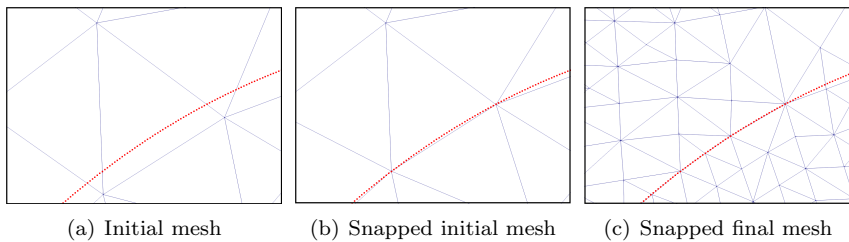


Fig. 7.2: (Example 7.1) A zoomed interface snapping from Figure 7.1

320 In Figure 7.3, we observe optimal convergence rates for the error, the residual-
 321 based and the recovered flux-based estimators. However, the efficiency index (i.e. the
 322 ratio between the estimator and the error) of η is more accurate than that of η_{res} .

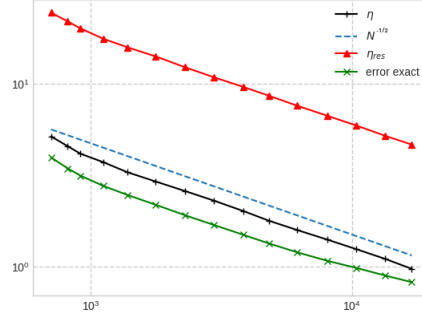


Fig. 7.3: (Example 7.1) Error convergence

EXAMPLE 7.2 (The L-shaped domain). *We now consider the L-shaped domain test, see for instance [26]. The domain is $\Omega = [-5, 5] \times [-5, 5] \setminus [0, 5] \times [-5, 0]$ and it presents again an interface, the circle centered at origin and of radius $\rho_0 = 2\sqrt{2}$. The exact solution is given in polar coordinates (ρ, θ) by:*

$$u(\rho, \theta) = \begin{cases} \rho^{2/3} \sin \frac{2\theta}{3}, & \text{if } \rho \leq \rho_0 \\ \rho_0^{2/3} \sin \frac{2\theta}{3} + \frac{2}{3\mu} \rho_0^{-1/3} \sin \frac{2\theta}{3} (\rho - \rho_0) & \text{otherwise} \end{cases},$$

whereas the diffusion coefficient k is defined as follows:

$$k(\rho) = \begin{cases} 1 & \text{if } \rho \leq \rho_0 \\ \mu & \text{otherwise} \end{cases}.$$

323 As stopping criteria in the AMR procedure, we now impose that the total number
 324 of degrees of freedom is less than 45000. The curved interface is treated as in the
 325 previous example, by snapping the mesh. Figure 7.4 shows a sequence of adapted
 326 meshes, while in Figure 7.5 one can see the convergence rates obtained for different
 327 values of μ , from 5 to 10000. As expected from the theoretical results, we numerically
 328 retrieve the robustness with respect to the jump of the diffusion coefficient.

EXAMPLE 7.3 (The Kellogg test). *We now consider the well-known checkerboard example, originally proposed by Kellogg [27]. Here, the line discontinuity of the diffusion coefficients meets the singularity of the solution. In addition, the coefficients are not quasi-monotone around the origin. The domain is $\Omega = [-1, 1]^2$, with two intersecting interfaces given by the lines $y = 0$ and $x = 0$. The diffusion coefficient is piecewise constant in each of the four sub-domains and is defined as follows:*

$$k(x, y) = \begin{cases} \kappa, & \text{if } xy \geq 0 \\ 1, & \text{otherwise} \end{cases}.$$

The exact solution is given by $u(r, \theta) = r^\delta \mu(\theta)$, with (r, θ) the polar coordinates centered at the origin and

$$\mu(\theta) = \begin{cases} \cos((\frac{\pi}{2} - \sigma)\delta) \cos((\theta - \frac{\pi}{2} + \rho)\delta), & 0 \leq \theta \leq \frac{\pi}{2} \\ \cos(\rho\delta) \cos((\theta - \pi + \sigma)\delta), & \frac{\pi}{2} \leq \theta \leq \pi \\ \cos(\sigma\delta) \cos((\theta - \pi - \rho)\delta) & \pi \leq \theta \leq \frac{3\pi}{2} \\ \cos((\frac{\pi}{2} - \rho)\delta) \cos((\theta - \frac{3}{2}\pi - \sigma)\delta) & \frac{3\pi}{2} \leq \theta \leq 2\pi \end{cases}.$$

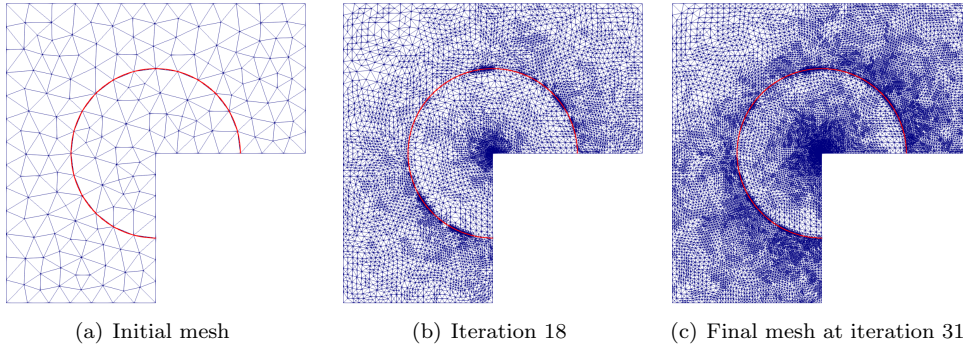


Fig. 7.4: (Example 7.2) Adaptive meshes

329 The solution has an infinite derivative at the origin and belongs to $H^{1+s}(\Omega)$ for any
 330 $s < \delta$. The numbers δ , σ , ρ and κ are related by some nonlinear relations. As
 331 in [28], we take $\delta = 0.1$, which yields $\sigma = -14.92256510455152$, $\rho = \frac{\pi}{4}$ and $\kappa =$
 332 161.4476387975881 .

333 As regards the AMR procedure, the stopping criteria is now that the relative error
 334 is less than 1%, which leads to 131 iterations. We present in Figure 7.6 a sequence of
 335 adapted meshes, starting from an initial mesh consisting of 8 triangles. One can see
 336 that the refinement takes place near the origin, as expected. The optimal convergence
 337 rates for the error and the estimators η and η_{res} are shown in Figure 7.7. Again, the
 338 efficiency index of η is asymptotically more accurate than that of η_{res} .

339 **EXAMPLE 7.4 (The Battery Problem).** Finally, we consider a problem attributed
 340 to I. Babuska, which can be found in [29], [30]; it models heat conduction in a battery
 341 with non-homogeneous materials. The domain is the rectangle $\Omega = [0, 8.4] \times [0, 24]$
 342 shown in Figure 7.8. The numbered regions show the areas of different materials; the
 343 location of the line segments that separate the regions can be found in [30].

344 The problem features a piecewise constant diffusion tensor $K = \begin{pmatrix} k_1 & 0 \\ 0 & k_2 \end{pmatrix}$ and
 345 mixed boundary conditions of Fourier-Robin type, $K\nabla u \cdot n + cu = g$ on $\partial\Omega$. Therefore,
 346 we have modified accordingly the discrete weak formulation and defined the boundary
 347 degrees of freedom $\sigma_h \cdot n$ as $\pi_h^m(g - cu_h)$. The definitions of the parameters ω^\pm and
 348 k_F in the tensor case is the same as in [25, 5]. The constants k_1 , k_2 and f for each
 349 region are given in Table 7.1. The boundary coefficients c and g are taken as follows:
 350 $c = g = 0$ on the left, $c = 1$ and $g = 3$ on the top, $c = g = 2$ on the right, and finally,
 351 $c = 3$ and $g = 1$ on the bottom.

k	k_1	k_2	f
1	25	25	0
2	7	0.8	1
3	5	0.0001	1
4	0.2	0.2	0
5	0.05	0.05	0

Table 7.1: (Example 7.4) The piecewise constant coefficient function K

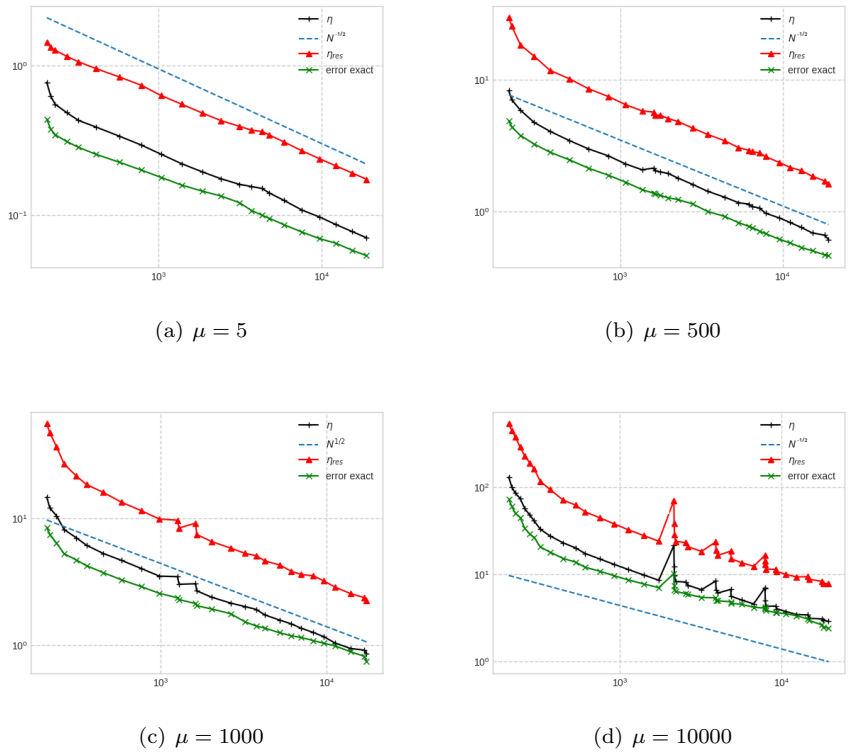


Fig. 7.5: (Example 7.2) Error convergence for different values of μ

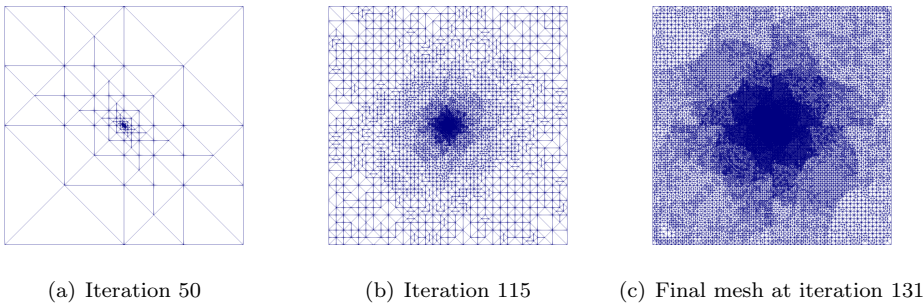


Fig. 7.6: (Example 7.3) Adaptive meshes

352 The exact solution is not known and has singularities at the points where three
 353 or more materials meet. For any $\varepsilon > 0$, there exists coefficients such that the solution
 354 is in $H^{1+\varepsilon}(\Omega)$; for the given set of coefficients, ε is about $1/2$.

355 We show in Figure 7.8 a sequence of adapted meshes. Figure 7.9 illustrates the
 356 interest of adaptive versus uniform mesh refinement. Besides the gain in the number

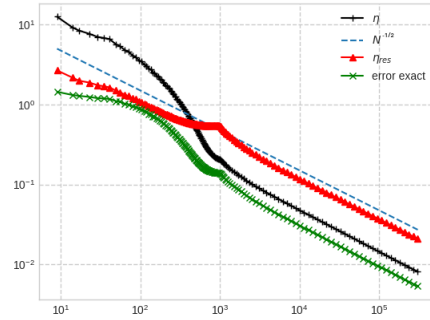


Fig. 7.7: (Example 7.3) Error convergence

357 of degrees of freedom and in computational time, the AMR procedure yields optimal
 358 convergence rate $O(h)$ whereas the uniform refinement only yields $O(h^{1/2})$.

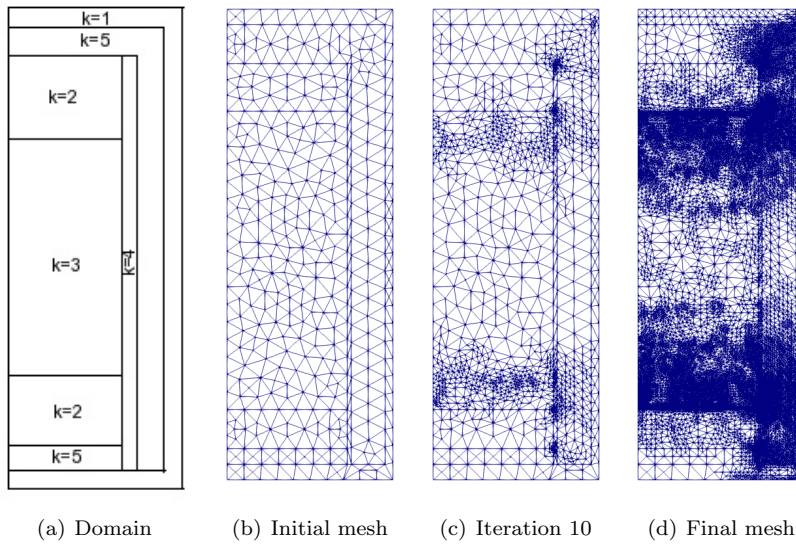


Fig. 7.8: (Example 7.4) sub-domains and adapted meshes

359 **8. Appendix: Proof of Lemma 3.3.** *Proof.* The proof follows the ideas of [10]
 360 for the Poisson equation. Let $\mu_h \in \mathcal{M}_h$. The idea is to construct $v_h \in \mathcal{D}_h^1$ associated
 361 to μ_h and satisfying

$$b_h(\mu_h, v_h) \gtrsim \|\mu_h\|_{\mathcal{M}_h}^2, \quad \|v_h\|_h \lesssim C_K \|\mu_h\|_{\mathcal{M}_h}. \quad (8.1)$$

362 The construction of v_h is done patch-wise. We look for $v_h = \sum_{N \in \mathcal{N}_h^{int}} v_N$ with
 363 v_N defined on ω_N . Let $N \in \mathcal{N}_h^{int}$ and let us define v_N , piecewise P^1 and discontinuous
 364 on ω_N , by imposing its values at the nodes of each triangle $T \in \omega_N$ as follows.

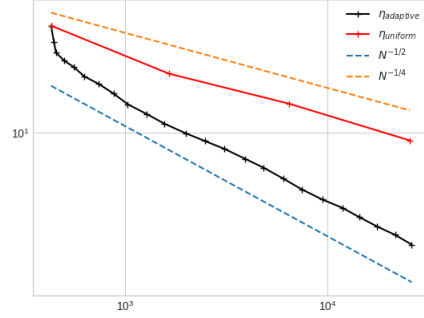


Fig. 7.9: (Example 7.4) Error convergence for adaptive and uniform refinements

At a node $M \neq N$ belonging to a side $F \in \mathcal{F}_N$ with $\{F\} = \partial T^+ \cap \partial T^-$, we set

$$(v_N)_{|T^\pm}(M) = 0 \quad \text{if } M \in \mathcal{N}_h^{int}.$$

365 If $M \in \mathcal{N}_h^\partial$, then we set

$$(v_N)_{|T^-}(M) = \delta_F |F| \mu_h|_F(M), \quad (v_N)_{|T^+}(M) = (\delta_F - 1) |F| \mu_h|_F(M), \quad (8.2)$$

where $\delta_F = 1$ if $k_{T^-} \leq k_{T^+}$ and $\delta_F = 0$ otherwise. This ensures that the definition of v_N is local and that

$$[v_N]_F(M) = 0 \quad \text{if } M \in \mathcal{N}_h^{int}, \quad [v_N]_F(M) = |F| \mu_h|_F(M) \quad \text{if } M \in \mathcal{N}_h^\partial.$$

366 Furthermore, one has that

$$k_{T^-} \delta_F^2 \leq 2k_F, \quad k_{T^+} (\delta_F - 1)^2 \leq 2k_F. \quad (8.3)$$

367 At the node N , we impose:

$$[v_N]_F(N) = |F| \mu_h|_F(N), \quad \forall F \in \mathcal{F}_N. \quad (8.4)$$

Thanks to the constraint imposed in the space \mathcal{M}_h , the linear system (8.4) is compatible, because we have:

$$\forall N \in \mathcal{N}_h^{int}, \quad \sum_{F \in \mathcal{F}_N} \mathfrak{s}_{N,F} [v_N]_F = \sum_{F \in \mathcal{F}_N} \mathfrak{s}_{N,F} |F| \mu_h|_F(N) = 0.$$

The construction of v_h yields that for any $F \in \mathcal{F}_h^{int}$ of vertices N and M , one has

$$[v_h]_F = [v_N]_F + [v_M]_F = |F| \mu_h|_F,$$

which yields

$$b_h(\mu_h, v_h) = \sum_{F \in \mathcal{F}_h^{int}} \frac{|F|^2 k_F}{2} \sum_{N \in \mathcal{N}_F} \mu_h|_F(N)^2 \simeq \int_{\mathcal{F}_h^{int}} |F| k_F \mu_h^2 = \|\mu_h\|_{\mathcal{M}_h}^2,$$

as well as

$$\sum_{F \in \mathcal{F}_h^{int}} \int_F k_F |F|^{-1} [v_h]^2 ds \lesssim \|\mu_h\|_{\mathcal{M}_h}^2.$$

Meanwhile, for a boundary side $F \in \mathcal{F}_h^\partial$ such that $F \in \partial\omega_N \cap \partial T$, one has that $v_h|_F = v_N|_F$ so one gets using (8.2) and (8.3) that

$$\int_F |F|^{-1} k_F v_h^2 ds \lesssim k_T \sum_{M \in \mathcal{N}_F} (v_N)|_T(M) \lesssim \sum_{F' \in \partial T \setminus \{F\}} \int_{F'} |F'| k_{F'} \mu_h^2 ds.$$

By summing upon the Dirichlet sides, it follows that

$$\sum_{F \in \mathcal{F}_h^D} \int_F k_F |F|^{-1} v_h^2 ds \lesssim \|\mu_h\|_{\mathcal{M}_h}^2.$$

368 In order to obtain (8.1), we still have to establish

$$\int_{\mathcal{T}_h} K \nabla v_h \cdot \nabla v_h dx \lesssim C_K^2 \|\mu_h\|_{\mathcal{M}_h}^2. \quad (8.5)$$

369 For this purpose, we need to specify the construction of v_N at the node N , that
 370 is to solve the system (8.4), which has a one-dimensional kernel (see [10, 21]). We fix
 371 one of the values of v_N in order to obtain (8.5) with the best constant C_K . We recall
 372 that n_N denotes the number of elements in ω_N and that the cells are numbered from
 373 T_1 to T_{n_N} , with T_1 the element such that $k|_{T_1} = \max_{T \subset \omega_N} k|_T$. We suppose (without
 374 loss of generality) that the triangles are ordered clockwise. For each $i \in \{1, \dots, n_N\}$,
 375 we set $F_i = \partial T_i \cap \partial T_{i+1}$ with $T_{n_N+1} = T_1$ and we recall that the sign coefficient
 376 $\mathfrak{s}_i := \mathfrak{s}_{N, F_i}$ equals 1 if $T_i = T^-$ with respect to F_i , and -1 otherwise. For the
 377 simplicity of notation, let us put $v_i := (v_N)|_{T_i}(N)$ and $\mu_i^* = \mathfrak{s}_i |F_i| \mu_h|_{F_i}(N)$. Noting
 378 that $[v_N]_{F_i} = \mathfrak{s}_i (v_i - v_{i+1})$ and that $\mathfrak{s}_i^2 = 1$, the system (8.4) can be written as follows:

$$v_i - v_{i+1} = \mu_i^*, \quad 1 \leq i \leq n_N - 1. \quad (8.6)$$

We choose $v_1 = 0$. Then (8.6) yields $v_i^2 \lesssim \sum_{j=1}^{i-1} (\mu_j^*)^2$, for $2 \leq i \leq n_N$. By using that

$$\frac{1}{k_{F_j}} = \frac{1}{k_j} + \frac{1}{k_{j+1}},$$

we next obtain that

$$k_i v_i^2 \lesssim \sum_{j=1}^{i-1} \frac{k_i}{k_{F_j}} k_{F_j} (\mu_j^*)^2 = \sum_{j=1}^{i-1} \left(\frac{k_i}{k_j} + \frac{k_i}{k_{j+1}} \right) k_{F_j} (\mu_j^*)^2, \quad 2 \leq i \leq n_N.$$

379 Recalling that $C_N = \max_{1 \leq j \leq i \leq n_N} \frac{\sqrt{k_i}}{\sqrt{k_j}}$ on ω_N , we have thus obtained:

$$k_i v_i^2 \lesssim C_N^2 \sum_{j=1}^{n_N-1} k_{F_j} (\mu_j^*)^2, \quad 1 \leq i \leq n_N. \quad (8.7)$$

One then has

$$\begin{aligned}
\int_{\mathcal{T}_h} K \nabla v_h \cdot \nabla v_h dx &\lesssim \sum_{T \in \mathcal{T}_h} \sum_{N \in \mathcal{N}_T} k_T (v_h)|_T^2(N) \\
&= \sum_{T \in \mathcal{T}_h} \sum_{N \in \mathcal{N}_T \cap \mathcal{N}_h^{int}} k_T (v_h)|_T^2(N) + \sum_{T \in \mathcal{T}_h} \sum_{N \in \mathcal{N}_T \cap \mathcal{N}_h^\partial} k_T (v_h)|_T^2(N) \\
&\lesssim \sum_{N \in \mathcal{N}_h^{int}} \sum_{T \in \omega_N} k_T (v_h)|_T^2(N) + \sum_{N \in \mathcal{N}_h^\partial} \sum_{T \in \omega_N} k_T (v_h)|_T^2(N).
\end{aligned}$$

Using (8.7) for the first right-hand-side term and (8.2), (8.3) for the second one, as well as the fact that $C_N \geq 1$, we finally get

$$\begin{aligned}
\int_{\mathcal{T}_h} K \nabla v_h \cdot \nabla v_h dx &\lesssim \sum_{N \in \mathcal{N}_h} C_N^2 \sum_{F \in \mathcal{F}_N} k_F |F|^2 \mu_h|_F^2(N) \\
&\lesssim C_\Omega^2 \sum_{F \in \mathcal{F}_h} k_F |F|^2 \sum_{N \in \mathcal{N}_F} \mu_h|_F^2(N) \simeq C_\Omega^2 \|\mu_h\|_{\mathcal{M}_h}^2
\end{aligned}$$

380 with $C_\Omega = \max_{N \in \mathcal{N}_h^{int}} C_N$. For K quasi-monotone, one has $C_N = 1$ for any node N and
381 hence, $C_\Omega = 1$. This ends the proof with $\beta \simeq C_\Omega^{-1}$. \square

REFERENCES

- 382
- 383 [1] P. Ladevèze and D. Leguillon. Error estimate procedure in the finite element method and
384 applications. *SIAM J. Numer. Anal.*, 20(3):485–509, 1983.
- 385 [2] M. Ainsworth and J. T. Oden. A posteriori error estimation in finite element analysis. *Comput.*
386 *Methods Appl. Mech. Eng.*, 142(1-2):1–88, 1997.
- 387 [3] L. H. Odsæter, M. F. Wheeler, T. Kvamsdal, and M. G. Larson. Postprocessing of non-
388 conservative flux for compatibility with transport in heterogeneous media. *Comput. Meth-*
389 *ods Appl. Mech. Eng.*, 315:799–830, 2017.
- 390 [4] P. Bastian and B. Rivière. Superconvergence and H(div) projection for discontinuous Galerkin
391 methods. *Int. J. Numer. Methods Fluids*, 42(10):1043–1057, 2003.
- 392 [5] A. Ern, S. Nicaise, and M. Vohralík. An accurate H(div) flux reconstruction for discontinuous
393 Galerkin approximations of elliptic problems. *C. R. Math.*, 345(12):709–712, 2007.
- 394 [6] D. Braess, V. Pillwein, and J. Schöberl. Equilibrated residual error estimates are p-robust.
395 *Comput. Methods Appl. Mech. Eng.*, 198(13-14):1189–1197, 2009.
- 396 [7] A. Ern, A. F. Stephansen, and M. Vohralík. Guaranteed and robust discontinuous Galerkin
397 a posteriori error estimates for convection–diffusion–reaction problems. *J. Comput. Appl.*
398 *Math.*, 234(1):114–130, 2010.
- 399 [8] Z. Cai and S. Zhang. Robust equilibrated residual error estimator for diffusion problems:
400 Conforming elements. *SIAM J. Numer. Anal.*, 50(1):151–170, 2012.
- 401 [9] A. Ern and M. Vohralík. Polynomial-degree-robust a posteriori estimates in a unified setting
402 for conforming, nonconforming, discontinuous Galerkin, and mixed discretizations. *SIAM*
403 *J. Numer. Anal.*, 53(2):1058–1081, 2015.
- 404 [10] R. Becker, D. Capatina, and R. Luce. Local flux reconstructions for standard finite element
405 methods on triangular meshes. *SIAM J. Numer. Anal.*, 54(4):2684–2706, 2016.
- 406 [11] W. Prager and J. L. Synge. Approximations in elasticity based on the concept of function
407 space. *Quart. Appl. Math.*, 5:286–292, 1947.
- 408 [12] L. Demkowicz and M. Swierczek. An adaptive finite element method for a class of variational
409 inequalities. In *Proceedings of the Italian-Polish Symposium of Continuum Mechanics*,
410 *Bologna*, 1987.
- 411 [13] J. T. Oden, L. Demkowicz, W. Rachowicz, and T. A. Westermann. Towards a universal hp
412 adaptive finite element strategy, Part 2. A posteriori error estimation. *Comput. Methods*
413 *Appl. Mech. Eng.*, 77(1-2):113–180, 1989.
- 414 [14] P. Destuynder and B. Métivet. Explicit error bounds in a conforming finite element method.
415 *Math. Comput.*, 68(228):1379–1396, 1999.

- 416 [15] M. Ainsworth and J. T. Oden. A unified approach to a posteriori error estimation using element
417 residual methods. *Numer. Math.*, 65(1):23–50, 1993.
- 418 [16] M. G. Larson and A. J. Niklasson. A conservative flux for the continuous Galerkin method
419 based on discontinuous enrichment. *Calcolo*, 41(2):65–76, 2004.
- 420 [17] T. Vejchodský. Guaranteed and locally computable a posteriori error estimate. *IMA J. Numer.*
421 *Anal.*, 26(3):525–540, 2006.
- 422 [18] D. Braess and J. Schöberl. Equilibrated residual error estimator for edge elements. *Math.*
423 *Comput.*, 77(262):651–672, 2008.
- 424 [19] R. Verfürth. A note on constant-free a posteriori error estimates. *SIAM J. Numer. Anal.*,
425 47(4):3180–3194, 2009.
- 426 [20] D. Cai, Z. Cai, and S. Zhang. Robust equilibrated a posteriori error estimator for higher order
427 finite element approximations to diffusion problems. *Numer. Math.*, 144(1):1–21, 2020.
- 428 [21] D. Capatina and C. He. Flux recovery for Cut Finite Element Method and its application in a
429 posteriori error estimation. *ESAIM: Math. Model. Numer. Anal.*, 55(6):2759 – 2784, 2021.
- 430 [22] G. Matthies and L. Tobiska. Inf-sup stable non-conforming finite elements of arbitrary order
431 on triangles. *Numer. Math.*, 102:293–309, 2005.
- 432 [23] M. Fortin and M. Soulie. A non-conforming piecewise quadratic finite element on triangles.
433 *Int. J. Numer. Methods Eng.*, 19(4):505–520, 1983.
- 434 [24] R. Verfürth. A posteriori error estimation and adaptive mesh refinement techniques. *J. Comput.*
435 *Appl. Math.*, 50(1-3):67–83, 1994.
- 436 [25] A. Ern, A. F. Stephansen, and P. Zunino. A discontinuous Galerkin method with weighted
437 averages for advection–diffusion equations with locally small and anisotropic diffusivity.
438 *IMA J. Numer. Anal.*, 29(2):235–256, 2009.
- 439 [26] A. Bonito, R. A. Devore, and R. H. Nochetto. Adaptive finite element methods for elliptic
440 problems with discontinuous coefficients. *SIAM J. Numer. Anal.*, 51(6):3106–3134, 2013.
- 441 [27] R. B. Kellogg. On the Poisson equation with intersecting interfaces. *Appl. Anal.*, 4(2):101–129,
442 1974.
- 443 [28] P. Morin, R. H. Nochetto, and K. G. Siebert. Data oscillation and convergence of adaptive
444 fem. *SIAM J. Numer. Anal.*, 38(2):466–488, 2000.
- 445 [29] L. Demkowicz. *Computing with Hp-adaptive finite elements, Vol. 1 : One and two dimensional*
446 *elliptic and Maxwell problems*. Chapman & Hall /CRC, 2007.
- 447 [30] W. F. Mitchell. A collection of 2D elliptic problems for testing adaptive grid refinement algo-
448 rithms. *Appl. Math. Comput.*, 220:350–364, 2013.